FEASIBILITY STUDY FOR AN ENHANCED GEOTHERMAL SYSTEM APPLICATION IN DIKILI-IZMIR REGION

A THESIS SUBMITTED TO
THE BOARD OF GRADUATE PROGRAMS
OF
MIDDLE EAST TECHNICAL UNIVERSITY, NORTHERN CYPRUS CAMPUS

BY

AYŞEGÜL TURAN

IN PARTIAL FULFILLMENT OF THE REQUIREMENTS

FOR

THE DEGREE OF MASTER OF SCIENCE

IN

SUSTAINABLE ENVIRONMENT AND ENERGY SYSTEMS PROGRAM

SEPTEMBER 2016

Approval of the Board of Graduate Programs

_____

Prof. Dr. Tanju MEHMETOĞLU
Chairperson

I certify that this thesis satisfies all the requirements as a thesis for the degree of Master of Science.

_____

Assoc. Prof. Dr. Ali MUHTAROĞLU
Program Coordinator

This is to certify that we have read this thesis and that in our opinion it is fully adequate, in scope and quality, as a thesis for the degree of Master of Science.

_____

Assist. Prof. Dr. Emre ARTUN
Supervisor

Examining Committee Members

Assoc. Prof. Dr. Ali MUHTAROĞLU, Jury Chair _____
Electrical and Electronics Engineering Prog., METU-NCC

Assist. Prof. Dr. Emre ARTUN, Jury Member _____
Petroleum and Natural Gas Engineering Prog., METU-NCC

Prof. Dr. Salih SANER, Jury Member _____
Petroleum and Natural Gas Engineering Prog., METU-NCC

Prof. Dr. Mahmut PARLAKTUNA, Jury Member _____
Petroleum and Natural Gas Engineering Dept., METU

Assist. Prof. Dr. Ceren İNCE, Jury Member _____
Civil Engineering Prog., METU-NCC

I hereby declare that all information in this document has been obtained and presented in accordance with academic rules and ethical conduct. I also declare that, as required by these rules and conduct, I have fully cited and referenced all material and results that are not original to this work.

Name, Last name: Ayşegül TURAN

Signature:

ABSTRACT

THE FEASIBILITY STUDY FOR AN ENHANCED GEOTHERMAL SYSTEM APPLICATION IN DIKILI-IZMIR REGION

TURAN, Ayşegül

MSc., Sustainable Environment and Energy Systems

Supervisor: Assist. Prof. Dr. Emre ARTUN

September 2016, 97 pages

For Turkey, one sustainable way to increase the clean energy share in the power generation can be the utilization of geothermal resources as they are abundant, reliable, domestic and able to provide base load. This study aims to investigate the untapped potential of hot dry rock systems to generate power. Dikili-İzmir geothermal field is selected as a case study with four different production scenarios. Accessible resource base and recoverable heat energy are calculated by employing a probabilistic approach- Monte Carlo simulation. The sensitivity analysis is done for the input reservoir parameters on heat potential. İzmir-Dikili geothermal field, having numerous hot springs with changing temperature from 30 °C to 100 °C, is currently only being utilized for district heating and greenhouse heating. In this thesis, in addition to the hydrothermal Yuntdağ volcanites system, Kozak hot dry rock system is suggested for direct and indirect utilization. Based on the existing accessible resource base and recoverable heat in place calculations, with 90% probability, the net electrical power can be produced from Kozak system is 8 MW_e and from Yuntdağ reservoir, it is 30 MW_e. Similarly, with 90% probability, the amount of net thermal power can be produced from Kozak system is 150 MW_t whereas Yuntdağ volcanites is capable of producing 850 MW_t. When unit volume

of reservoirs are considered, with 90% probability, Kozak can produce 3.8 times of what Yuntdağ can produce in terms of electricity generation. For net thermal power, Kozak can produce 2.6 times of Yuntdağ. Sensitivity analysis showed that reservoir area, rock-fluid temperature and recovery factor, ranked as top three among the seven input parameters, have the greatest impact on net power output. Sustainability attributes of the discussed cases are evaluated in terms of saved CO_2 amount and saved money by employing a domestic energy source rather than an imported one. The present work extends the previous work by considering hot dry rock systems as an alternative reservoir. Further, none of the previous geothermal resource assessment studies highlight the sustainability attributes but present study analyzes them in an economical and environmental point of view.

Keywords: Geothermal, Hot Dry Rock Systems, Enhanced Geothermal Systems, Resource Assessment, İzmir-Dikili.

ÖZ

DİKİLİ-İZMİR BÖLGESİNDE GELİŞTİRİLMİŞ JEOTERMAL SİSTEMİ UYGULAMASI İÇİN FİZİBİLİTE ÇALIŞMASI

TURAN, Ayşegül

Yüksek Lisans, Sürdürülebilir Çevre ve Enerji Sistemleri Programı

Tez Yöneticisi: Y. Doç. Dr. Emre ARTUN

Eylül 2016, 97 sayfa

Türkiye için enerjide dışa bağımlılığı azaltmanın sürdürülebilir bir yolu jeotermal kaynakların elektrik üretimine katkısının arttırılması olabilir. Bu çalışmada, kızgın kuru kaya sistemlerinin bugüne kadar Türkiye'de değerlendirilmeyen potansiyeli, İzmir-Dikili jeotermal sahası örneğiyle, elektrik ve ısı üretimi için önerilmektedir. İzmir-Dikili jeotermal sahası, sıcaklıkları 30 °C ile 100 °C arasında değişen sıcak su kaynakları ile günümüzde sadece konut ve sera ısıtma amaçlı kullanılmaktadır. Bu çalışmada, alandaki Yuntdağ volkanitlerinin oluşturduğu hidrotermal rezervuarın yanı sıra Kozak kızgın kuru kaya rezervuarından da ısıtma ve elektrik üretme amaçlı faydalanabileceği görülmüştür. Monte Carlo simülasyonu kullanılarak yapılan kaynak değerlendirmesi çalışmaları sonucunda, sahanın yerinde net elektrik gücü, %90 olasılıkla, Kozak kızgın kuru kaya sisteminden 8 MW_e; Yuntdağ hidrotermal rezervuarından 30 MW_e olarak hesaplanmıştır. Benzer şekilde sahanın yerinde net ısıl gücü, %90 olasılıkla, Kozak sisteminden 150 MW_t ve Yuntdağ sisteminden 850 MW_t olarak hesaplanmıştır. Rezervuarların birim hacimlerinden elde edilebilecek net ısıl güç ve elektrik güçleri karşılaştırıldığında, %90 olasılıkla, Kozak sisteminin Yuntdağ sisteminin sırasıyla 2.6 ve 3.8 katı üretim yapabileceği görülmüştür. Bu hesaplamalarda sonuca en çok etki eden ilk üç verinin rezervuar alanı, rezervuar sıcaklığı ve kurtarma faktörü olduğu görülmüştür. Elde

edilen sonuçların sürdürülebilirlik açısından değerlendirilmesi, korunan karbondioksit miktarı ve doğal gaz gibi ithal edilen enerji kaynaklarının elektrik üretimindeki payının azaltılmasının ülke ekonomisine etkisi şeklinde yapılmıştır. Bu çalışma önceki çalışmalardan farklı olarak Kozak kızgın kuru kaya sistemini, Yuntdağ hidrotermal sistemiyle dört farklı üretim durumu üzerinden kıyaslar. Ayrıca daha önce bu alanda yapılan çalışmalardan farklı olarak elde edilen sonuçları sürdürülebilirlik kavramı üzerinden değerlendirir.

Anahtar Kelimeler: Jeotermal, Kızgın Kuru Kaya Sistemleri, Geliştirilebilir Jeotermal Sistemler, Kaynak Değerlendirmesi, İzmir-Dikili.

To My Family

ACKNOWLEDGMENTS

I want to express my deepest gratitude to my supervisor Assist. Prof. Dr. Emre ARTUN for his kind guidance and advice. I am honored to be his first graduate student.

I would like to thank Prof. Dr. Salih SANER for his criticism and encouragements during not only my research but also my teaching assistantship.

I would like to express my special thanks to Prof. Dr. Mahmut PARLAKTUNA for his assistance and significant contributions.

I am grateful to Assist. Prof. Dr. Doruk ALP for his support, comments and inspiration.

I would like to deeply thank Gözde BİLGİN, Görkem EKEN and Beste ÖZYURT from Ankara campus for their support that did not leave me alone in Northern Cyprus campus.

TABLE OF CONTENTS

LIST OF TABLES

LIST OF FIGURES

LIST OF ABBREVIATIONS

CDF: Cumulative Distribution Function

EGS: Enhanced Geothermal System

GEPA: Atlas of Solar Energy Potential

GEPP: Geothermal Energy Power Plant

HDR: Hot Dry Rock

IDDP: Icelandic Deep Drilling Project

MTA: General Directorate of Mineral Research and Exploration

MWe: Megawatt-electricity

MWt: Megawatt-thermal

NEP: Net Electrical Power

NTP: Net Thermal Power

ORC: Organic Rankine Cycle

PDF: Probability Distribution Function

RFT: Rock-Fluid Temperature

RHE: Recoverable Heat Energy

STD. DEV.: Standard Deviation

CHAPTER 1

INTRODUCTION

1.1 Project Overview

Through the human history, engineering has contributed to the advance of civilization. Starting from the ancient ages, innovations of engineers have had an earth-shattering effect on world's people. The marvels of Modern era were machines, steam engine facilitated mining, powered trains and ships, whereas the great achievements of 20th century were widespread distribution of clean water and electricity, and internet. With the development of telecommunication, the accomplishments in all branches of science became largely universal, timely parallel and relatively globally-available. Within all of these advances, the problem of sustaining the needs of growing population, to ensure the 'future' with the finite resources of Earth, has occurred [1].

The increase in the concentration of CO_2 released to the atmosphere leads to the average temperature rise which has resulted in melting of polar ice caps and the extreme weather events seen worldwide. They are basically the evidences of Earth's disturbed balance. In other words, 7.349 billion people -world population as of 2015 [2] - consume and pollute far more than Earth can sustain. Thus the grand challenges that wait the engineers of 21st century highlight the need to develop new sources of energy while reversing the degradation of environment [1].

Expanding the options among clean energy sources (solar, wind, wave, etc.), one other potential source may be the Earth's internal heat, namely geothermal energy. It is inexhaustible, abundant, reliable and with relatively less emissions or environmental impact. Further, different than the other renewable energy conversion technologies, geothermal exploitation is an already approved technology since it is based on experience derived from oil and gas industry. It can be a feasible way to increase the renewable sources' share in energy supply for those areas lucky enough to find themselves on top of it like Turkey. In addition to heat source existence, natural or artificial heat transfer schemes are needed for a successful exploitation. Increased development activity in today's geothermal market has drawn attention to non-conventional technologies such as enhanced geothermal systems (EGS). EGS may

create entirely new geothermal fields that were once omitted due to low permeability, lack of fluid and/or insufficient flow rate.

This thesis aims to assess the possibilities in Turkey for employing new technologies in geothermal energy, specifically in hot dry rock (HDR) systems where geo-fluid is absent and the permeability is very low. Employing such a carbon-free source can help to combat climate change by lowering the extensity of fossil fuel combustion. HDR systems may be an alternative to the dispersed nature and low to medium enthalpy of hydrothermal geothermal systems in Turkey. The encouraging results may allay the concerns of investors and decision makers about the high cost of drilling and untapped potential of HDR geothermal resources.

1.2. Motivation

Turkey, strategically positioned at the crossroads of Asia, Europe and the Middle East, is heavily dependent on expensive imported energy sources such as natural gas and crude oil that place a big burden on Turkish economy. On the other hand, air pollution has become a great environmental concern since these sources provide energy through combustion. With the increasing energy demand mainly caused by Turkey's economic growth rate that peaked as 9.2% in 2010 in the last ten years (as of the third quarter of 2015, it is 4%) [3], sustainable supply became a problem which cannot be ignored. As a solution, a major renewable energy and energy efficiency program has been embarked in the country. The target is set to increase clean energy share at least to 30% of Turkey's power supply by 2023-the 100th anniversary of Turkish Republic. Another goal stated in the strategy paper of security supply is to decrease natural gas share in power supply to 30% [4]. As of 2014, it was 47.9% [5].

When location based motivation considered, according to the 2013 statistics, 90.48% of the total net electrical power was supplied by natural gas in İzmir. Wind, that has an intermittent nature, the only renewable energy source utilized in İzmir for electricity generation, contributed to the total production with a 6.99% share. Fuel oil provided 2.45% and waste gas provided 0.08% of production [6]. Thus, the share of renewable energy sources in the power generation, should be increased in the region.

When it comes to the consumption, as of 2013, the electricity consumption is 17,657,930 MWh in İzmir. It corresponds to the 7.2% of Turkey's total consumption. However, in İzmir, electricity consumption per person is 4,348 kWh which is 35.8% more than Turkey's average [6]. The reason behind this fact may be the heavy use of cooling due to hot weather conditions.

As a further recommendation, ground sourced geothermal heat pumps can be utilized to decrease the share of cooling via electricity in consumption.

About 60% of geothermal energy utilized in İzmir is used for district heating. Greenhouse heating corresponds to around 35%. Thermal tourism has a 5% share [6]. It means that all of the utilized geothermal energy sources in İzmir are directly-utilized. In other words, none of them are used for electricity generation. This study suggests the untapped potential of hot dry rock systems to increase the share of geothermal in power production.

The motivation behind the present study is to contribute to the achievement of aforementioned objectives by narrowing the gap in the literature and highlighting the ignored electricity production capacity of hot dry rock geothermal resources. Since geothermal energy requires no storage system and it can support baseload (in other words it can run 24 hours a day), geothermal resources are hence preferred over other intermittent renewable energy resources such as wind and solar.

1.3. Geothermal Exploration and Applications in Turkey

In the world, many countries have significant geothermal resources depending on their locations with respect to plate tectonics. These places are along 'Ring of Fire' (i.e. a geographical area of high volcanic and seismic activity caused by tectonic plate boundaries.), 'spreading centers, continental rift zones and other hot spots'. Turkey is one of these countries. It is located on the Mediterranean part of Alpine-Himalayan Tectonic Belt, which is a young belt presenting important geothermal potential. The horst-graben system and widespread volcanism in the Western Anatolia, active tectonics in the Central and Eastern Anatolia and right lateral-strike slip North Anatolian Fault Zone affect the distribution of the geothermal regions in the country as seen in Figure 1 [7].

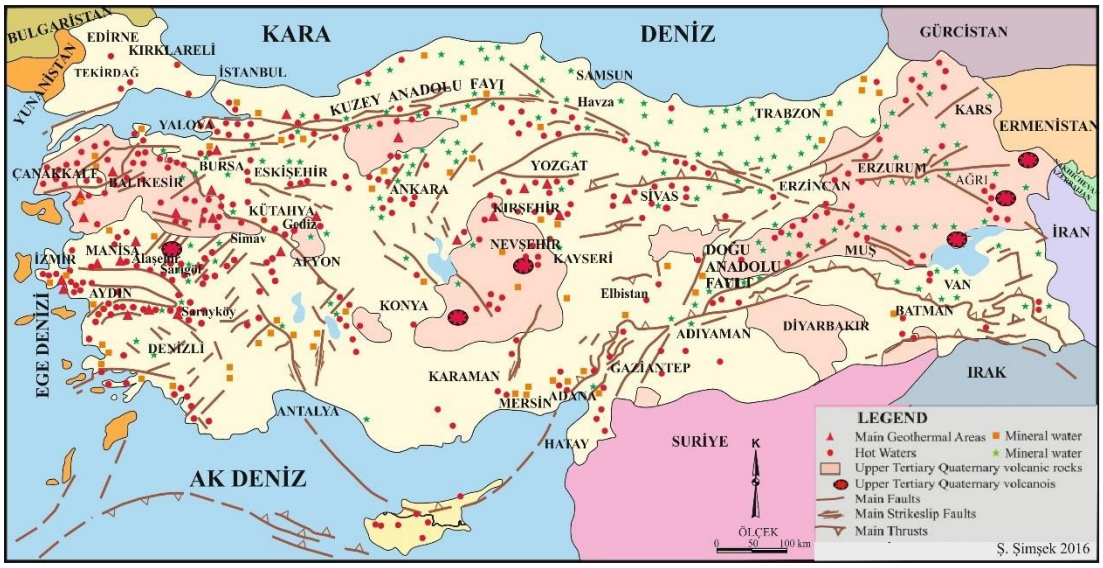

Figure 1: Distribution map of geothermal resources in Turkey with respect to plate tectonics [7].

Parallel to its potential, Turkey is not a new player in the geothermal energy market. General Directorate of Mineral Research and Exploration (MTA) started geothermal resource exploration in 1960's in Turkey. The first geothermal power plant, Kızıldere, was installed in 1984. However, these studies came to a standstill due to improper policies. With the new millennium, global ambition to decrease CO_2 emissions increased. Kyoto protocol, an international agreement contract that places restrictions on countries to reduce the emission of greenhouse gases, was put into operation in 2005. Turkey signed Kyoto protocol in August 2009 [8]. Increase in the fuel prices, peaked in 2008, became another accelerator to switch to renewable energy sources.

In 2005, related changes have started to be done in energy laws. Law no. 5346 was put into force in 10.05.2005. This law includes the extensification of power generation from renewable energy sources, increasing diversity of energy sources, decreasing greenhouse gas emissions, waste disposal, environmental protection and the development of the industries which help to achieve these targets [9].

Electricity production from renewable energy sources is supported by law no. 6094 that was put in place on 29.12.2010. In accordance with law no. 5346, the feed in tariff for electricity generated by geothermal energy is 10.5 US $ cent/kWh [10]. The government incentives and the growth potential started to draw attention to Turkey. Foreign investors have started to see major business development opportunities not only in geothermal but also in solar, wind,

hydro and all elements of energy efficiency. Over $40 billion investment is expected in this area by 2020 [11].

Table 1 clearly shows the effect of the new law about the utilization of renewable energy sources in power production on specifically geothermal electricity production capacity of Turkey [12]. In Table 1, the second column represents the difference in capacity (MW_e) between the years 2005-2010. Similarly, the difference in produced energy between the years 2005-2010 is given in units of GWh in the third column.

Table 1: Top 5 countries in terms of increase in electricity production from geothermal in years 2005-2010 [12] (all values are the amount of increase in electricity production either as in units of MW_e, GWh or as percentage).

Country	MW_e	GWh	$\%MW_e$	%GWh
USA	496	-2.314	19	-14
Indonesia	400	3.515	50	58
Iceland	373	3.114	184	210
New Zealand	193	1.281	44	46
Turkey	62	385	308	368

In years 2010-2015, geothermal development has risen even quicker, compared to 2005-2010, towards an impressive growing point and Turkey became the first-ranked country in the world for absolute increase as 539% in GWh and 336% in MW_e [13].

The number of the geothermal sites, which can be economically utilized, in Turkey is 227. The number of the hot and mineral water resources is about 2,000. The (spring or well discharge and/or reservoir) temperature range of these sources is 20-287 °C [14]. Figure 2 shows the temperature pattern of those geothermal sites and their utilization ways. Low temperature sites are shown by blue color whereas high temperature sites are represented by red color. As seen in Figure 2, the number of geothermal sites utilized for heating purposes is greater than for power production. Only 10 districts (namely; Aydın-Nazilli, Yılmazköy, Kuyucak, Sultanhisar, Germencik, Köşk, İncirliova, Çanakkale-Ayvacık, Denizli-Sarayköy, and Manisa-Alaşehir) are being utilized for electricity generation in Turkey and all of them are located in Western Anatolia as can be seen in Figure 1 [14]. It is an indicator of the fact that the majority of Turkey's hydrothermal resources are low enthalpy resources. In other words, their ability to do thermodynamic work are low.

Armstead has classified geothermal fields into semi-thermal fields (produces hot liquid up to 100 °C at the surface), hyper-thermal wet fields (produces hot liquid and gas at the surface) or hyper-thermal dry fields (produces dry saturated or superheated steam)' in addition to the enthalpy-based classification chart for geothermal systems given in Table 2 [16]. The temperature ranges in the classification chart are not certain; in other words they are not yet generally agreed upon.

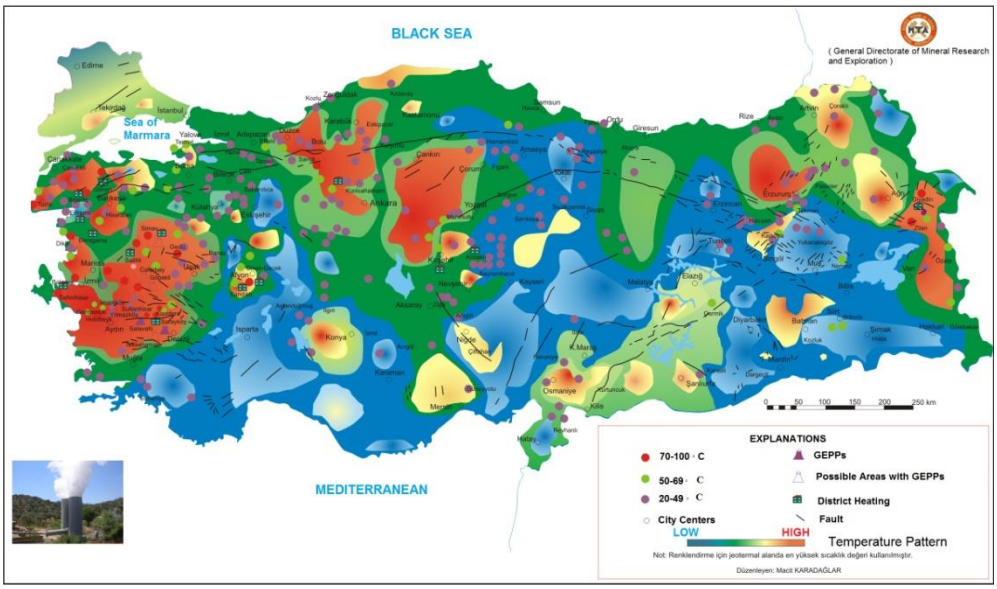

Figure 2: Map of temperature pattern of geothermal resources in Turkey and their utilization ways [15].

In Turkey, low enthalpy resources' utilization has been almost restricted to balneology, greenhouse heating and district heating. That carried Turkey to top-ranks in related worldwide lists as stated in Table 3 while its total installed capacity is 2,886.3 MW_t and annual energy use 45,126 TJ/yr, as stated in Table 4 [17]. Nevertheless, regarding indirect utilization ways, Turkey cannot be seen among top five countries (USA, Philippines, Indonesia, Mexico, New Zealand; respectively) worldwide [12]. As of September 2016, there are 23 licensed geothermal electricity power plants (GEPP) in operation with a total capacity of 584.658 MW_e. The total number of all different-staged GEPPs with in force licenses is 36, with a total capacity of 1,014.598 MW_e [19]. Names of the companies, locations and other details are listed in Table 5. It means that Turkey needs to find solutions to increase indirect utilization of geothermal resources. It can be achieved either implementing hybrid energy systems to

increase the enthalpy of source or focusing on EGS which is the major development direction of future geothermal energy utilization.

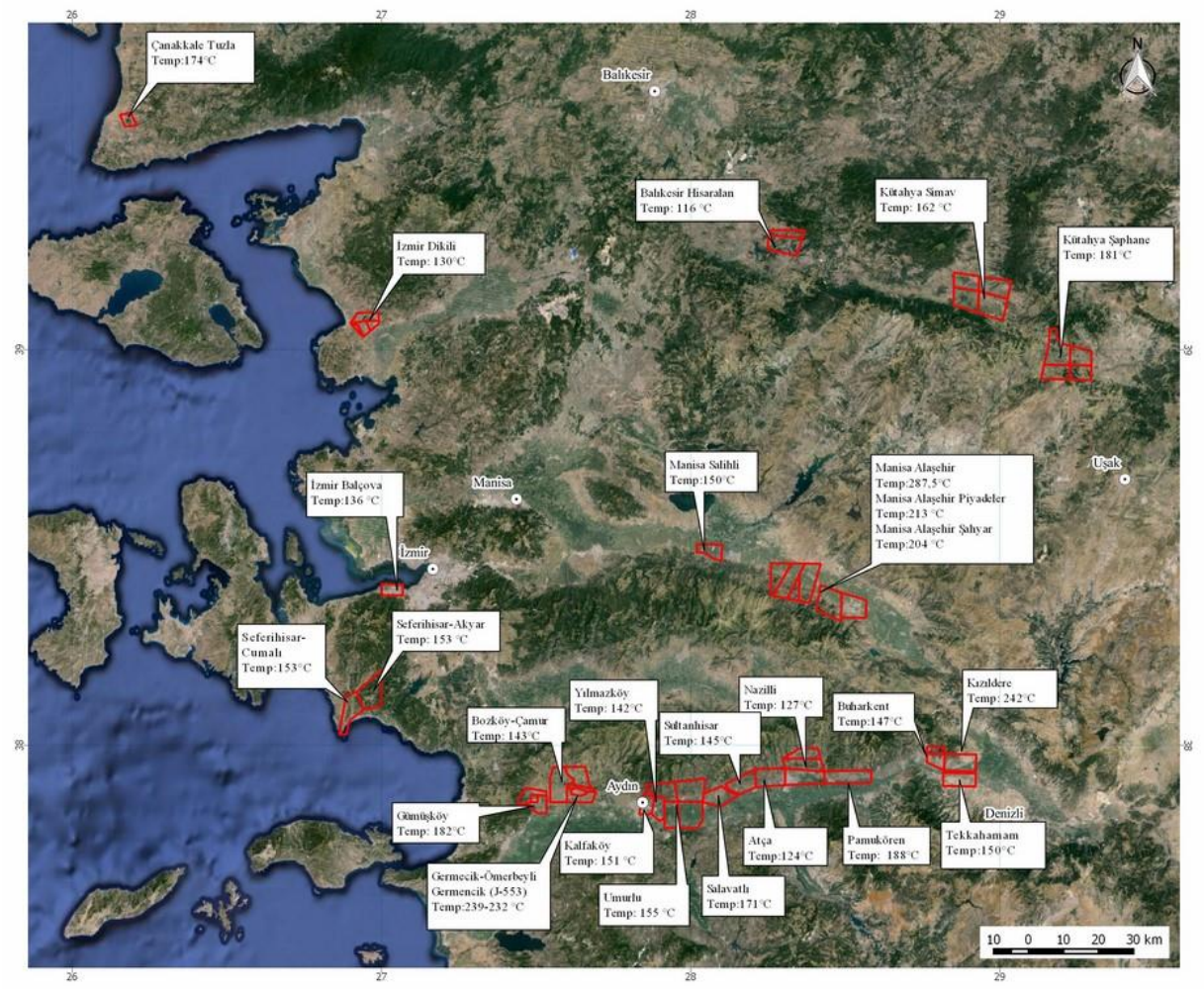

Figure 3: Map of geothermal sites utilized for power production in Turkey [18].

Table 2: Classification of hydrothermal resources based on temperature [20].

	Muffer and Cataldi (1978)	Hochstein (1988)	Benderitter and Cormy (1990)	Haenel et al. (1988)
Low Enthalpy	<90 °C	<125 °C	<100 °C	<150 °C
Intermediate	90 °C-150 °C	125 °C-225 °C	100 °C-200 °C	-
High Enthalpy	>150 °C	>225 °C	>200 °C	>150 °C

Table 3: The top five countries in different direct applications of geothermal resources [17].

Balneology	Greenhouse Heating	District Heating
China	**Turkey**	China
Japan	Russia	Iceland
Turkey	Hungary	**Turkey**
Brazil	China	France
Mexico	Netherlands	Germany

Table 4: Total installed capacity and annual energy use in direct use applications of geothermal resources in Turkey [17].

	Total Installed Capacity in MW_t	Annual Energy Use in TJ/yr
Greenhouse Heating	612	11,580
Individual Space Heating	420	4,635
District Heating	805	8,885
Geothermal Heat Pumps	42.8	960
Bathing &Swimming	1,005	19,106
Agricultural Drying	1.5	50

1.4. Research Problem and Thesis Objectives

For Turkey, one of the sustainable ways to increase the clean energy share in the power generation is the utilization of untapped geothermal resources. The subject of this thesis roots from the common existence of young volcanic regions that are the geothermal environments with high heat flow, low permeability and no water. With today's technology, the enhanced geothermal system (EGS) is the best energy conversion system to exploit these resources, by circulating water through wells in artificially fractured hot rock, both from a technical and environmental point of view. In this study, four different scenarios were defined to see which geothermal system in Dikili region can be utilized more feasibly. These scenarios are the direct and indirect utilizations of Yuntdağ Volcanites (as a hydrothermal geothermal system) and Kozak pluton (as EGS). The conducted feasibility study is based on the results of the heat in place calculation and sensitivity analysis of input parameters. It also takes the comparison of carbon emissions of each discussed system into account. For geothermal resource assessment, volume method was applied to calculate thermal energy contained in a given volume of rock and fluid and to estimate how much of this energy is recoverable. A probabilistic study is carried out rather than a deterministic one since the nature of the uncertainty of input parameters is described with probability density functions. Thus, the heat in place calculation is carried out by utilizing Monte Carlo simulation. The impact of the sensitivity of input parameters such as porosity, formation volume, rock and fluid temperature, fluid density, and recovery factor on heat generation was also investigated. All analyses were carried out for İzmir-Dikili geothermal site. The objective of the study is to find out the optimum utilization for Dikili geothermal resources whose potential has not been fully evaluated.

Table 5: Different staged GEPPs in Turkey as of September-2016 with a total capacity (capacity in operation + capacity under construction) of 1014.598 MW_e [19].

Company Name	**GEPP Name / Location**	**Capacity under Construction (MW_e)**	**Capacity in Operation (MW_e)**	**Total Capacity (MW_e)**
Akça Enerji	Tosunlar 1 JES/ Sarayköy-Denizli	0	3,807	3,807
İn-Altı Termal	Gök JES / Sarayköy-Denizli	3	0	3
Menderes Geothermal	Dora-4 JES/ Köşk-Aydın	0	17	17

Table 5: Different staged GEPPs in Turkey as of September-2016 with a total capacity (capacity in operation + capacity under construction) of 1014.598 MW_e [19]. (cont'd)

Company Name	GEPP Name / Location	Capacity under Construction (MW_e)	Capacity in Operation (MW_e)	Total Capacity (MW_e)
Karkey Karadeniz	Karkey Umurlu JES/ Köşk-Aydın	0	12	12
Ken Kipaş	Ken Kipaş JES/ Yılmazköy-Aydın	0	24	24
Maren Maraş	Deniz (Maren 2) JES/ Germencik-Aydın	0	24	24
Mtn Enerji	Babadere JES/ Ayvacık-Çanakkale	0	8	8
Türkerler Jeotermal	Türkerler Alaşehir JES/ Alaşehir-Manisa	0	24	24
Jeoden Elektrik	Jeoden/ Sarayköy-Denizli	2.52	0	2.52
Zorlu Jeotermal	Alaşehir JES/ Alaşehir- Manisa	0	45	45
Kiper Elektrik	Kiper JES/ Nazilli-Aydın	20	0	20
Çelikler Jeotermal	Sultanhisar JES/ Sultanhisar-Aydın	13.8	0	13.8
Çelikler Jeotermal	Pamukören JES 3/ Kuyucak-Aydın	0	22.51	22.51
Çelikler Pamukören Jeotermal	Pamukören JES 2/ Kuyucak-Aydın	0	22.51	22.51
Gümüşköy Jeotermal	Gümüşköy JES/ Germencik-Aydın	0	13.2	13.2
Menderes Geothermal	Dora-2 JES/ Köşk-Aydın	0	9.50	9.50
Sanko Enerji	Sanko JES/ Salihli-Manisa	15	0	15
Gürmat Elektrik	Efeler JES İncirliova-Aydın	47.4	114.9	162.3
Menderes Geothermal	Dora-3 JES/ Köşk-Aydın	0	34	34
Maren Maraş Elektrik	Maren Santrali/ Germencik-Aydın	0	44	44
Zorlu Doğal Elektrik	Kızıldere JES/ Sarayköy-Denizli	0	15	15
Menderes Geothermal	Dora-1/ Sultanhisar-Aydın	0	7951	7951

Table 5: Different staged GEPPs in Turkey as of September-2016 with a total capacity (capacity in operation + capacity under construction) of 1014.598 MW_e [19]. (cont'd)

Company Name	GEPP Name / Location	Capacity under Construction (MW_e)	Capacity in Operation (MW_e)	Total Capacity (MW_e)
Tuzla Jeotermal	Tuzla/ Ayvacık-Çanakkale	0	42497	42497
Gürmat Elektrik	Galip Hoca JES/ Germencik-Aydın	0	47.4	47.4
Bereket Jeotermal	Kızıldere/ Sarayköy-Denizli	0	31199	31199
Zorlu Doğal Elektrik	Kızıldere 2 JES Sarayköy-Denizli	0	80	80
Maren Maraş	Kerem JES Germencik-Aydın	0	24	24
Greeneco	Greeneco JES/ Sarayköy-Denizli	12.8	12.8	25.6
Enerjeo	Enerjeo Kemaliye Santrali/ Alaşehir-Manisa	0	24.9	24.9
Çelikler Jeotermal	Pamukören JES/ Kuyucak-Aydın	0	67.53	67.53
Mis Enerji	Mis-1/ Alaşehir-Manisa	15	0	15
Sis Enerji	Özmen-1 JES Alaşehir-Manisa	23.52	0	23.52
Türkerler Jeotermal	Alaşehir JES 2 Alaşehir-Manisa	24	0	24
Zorlu Doğal Elektrik	Kızıldere-3 JES Sarayköy-Denizli	95.2	0	95.2
Turcas Kuyucak Jeotermal	Kuyucak JES Kuyucak-Aydın	18	0	18
Karkey Karadeniz	Umurlu-2 JES Köşk-Aydın	12	0	12

1.5. Contribution of the Study

When the energy sector started to draw more attention after 2005, the number of the academic studies increased obviously [21]. Another reason may be the fact that oil bust has turned out as geothermal boom. Main topics are performance analyses on different thermodynamic cycles, numerical modelling studies and resource assessments. Some of the prominent master

theses on geothermal power production are as follows: Halaçoğlu (2015) focuses on performance analysis of Kızıldere-2 Geothermal Power Plant. Ünverdi (2011) conducts a similar study for Germencik Geotermal Power Plant. Karagüç (2013) evaluates the geothermal potential in Balıkesir and its economic impacts. Karadaş (2013) assesses the performance of a binary cycle geothermal power plant. Similarly, Wirawan (2015) analyzes the performance of Darajat dry-steam geothermal power plant unit-1. Aydın (2015) presents a study about optimization of electricity generation from geothermal resources by combining flash and binary systems. Süren (2012) analyzes energy and exergy on geothermal systems when flash vapor and binary systems are in conjunction. Günay (2012) conducts a numerical modelling study on Edremit geothermal field [21].

Most relevant studies, including resource assessment conducted for geothermal sites in Turkey, are Avşar (2011), Atmaca (2010), and Arkan et al. (2005) [21]. Atmaca (2010) which is on the same research track with this master thesis conducts a resource assessment in Aydın-Pamukören geothermal field. Similarly, in these three studies, volumetric method is employed and Monte Carlo simulation technique is used for resource assessment of conventional geothermal resources in Edremit, Pamukören, and Balçova respectively. Only in Balçova resource assessment study, sensitivity analysis was conducted by a different method (regression charts) that is employed in this thesis (tornado charts). Sustainability attributes of the studies are not mentioned in terms of neither carbon emissions nor economic analysis.

None of the aforementioned studies is about HDR geothermal systems. To our knowledge, this is the first academic study that suggests HDR geothermal systems for electricity. As a case study, the proposed approach is implemented for an area in İzmir-Dikili, in Western Anatolia, and a net power output is calculated. The comparison is done between traditional geothermal systems i.e. hydrothermal and nonconventional ones, i.e. EGS. The results can assist authorities during decision making process. Further, this study is also an opportunity to summarize what has been done and to suggest what should be done in Turkish geothermal energy sector.

1.6. Thesis Content

This thesis is composed of five chapters:

Chapter 1, which is introduction, prepares the reader for the conducted study. It states the research problem, summarizes the current situation in geothermal energy in Turkey, explains the motivation behind this study and describes the methodology of the study briefly.

Chapter 2 presents literature review related to geothermal systems, their utilization ways and new energy conversion technologies, specifically Hot Dry Rock systems, which are recently gaining momentum worldwide. This chapter also focuses on Dikili geothermal site.

Chapter 3 explains the methodology which is employed during resource assessment of Dikili geothermal field.

Chapter 4 discusses the results in economic and environmental aspects by calculating the saved amount of money and CO_2 by employing a domestic energy source like geothermal.

Chapter 5 draws conclusions and presents suggestions for future studies.

CHAPTER 2

LITERATURE REVIEW

Geothermal energy is the thermal energy stored within Earth's crust. It is a renewable energy source when the amount of heat extracted is compared to the heat potential of Earth. Its sustainability can be ensured by reinjection of the geo-fluid after its heat is utilized. Geothermal reinjection provides an additional recharge to the reservoir and an environmentally friendly solution to the waste water disposal. Reinjection also reduces the pressure decline in the geothermal reservoirs.

2.1. Geothermal Systems

Systems in which Earth's interior heat is sufficiently concentrated to form an energy source are called geothermal systems. They can be classified based on the heat source, geological and hydrogeological characteristics of the environment [23, 24]. In this study, geothermal systems are mainly classified as hydrothermal and advanced systems:

Hydrothermal systems are the traditional, well studied geothermal resources. They contain hot steam and/or water. That geo-fluid, which has been shown as cold meteoric water in Figure 4, is the way of heat convection in hydrothermal systems. Hydrothermal systems are seen in high porosity-high permeability environments and are heated by shallow young, magmatic intrusions as seen in Figure 4. Heated geo-fluid is carried along faults, shown as black solid lines in the related figure, close to the surface. In these systems, reservoir temperature and flow capacity are naturally sufficient for production. These systems feed the main geothermal production of today's world. Similarly in Turkey the geothermal fields that have been utilized so far are hydrothermal systems.

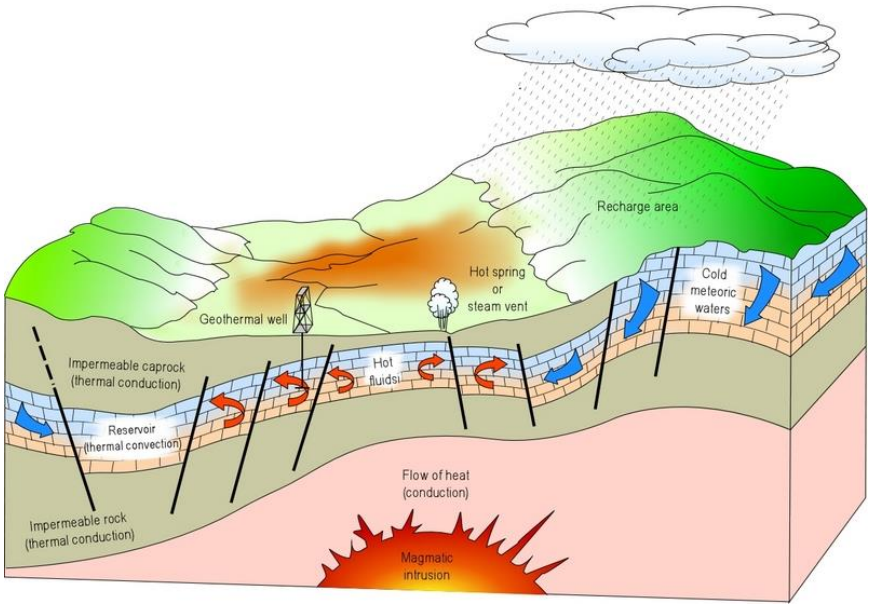

Figure 4: Conceptual model of a hydrothermal system [22].

On the other hand, advanced geothermal systems are the nonconventional ones, developing with advancing in reservoir engineering and drilling technology. These systems are geo-pressured, magma and hot dry rock (HDR) systems [23]:

Geo-pressured system forms in a basin in which very rapid sedimentation occurs yielding in high pressure geo-fluid. It is commonly seen in deep sedimentary basins [23].

Magma is another advanced geothermal system that can be utilized with the recent advances in technology. At several volcanic locations, magma exists within the top 5 km of crust [23]. Eventually magma is the source of all high-temperature geothermal resources. If this heat energy from magma is harvested, it constitutes a lot to the today's 'global energy inventory'. Up to now, it has not been achieved due to practical difficulties such as drilling material restrictions. However, Icelandic Deep Drilling Project (IDDP) became world's first magma-EGS created as announced on January 2014 [25]. Figure 5 shows the schematic illustration of IDDP project. The magma intrusion seen in the figure gives rise to the formation of a reservoir at supercritical conditions which compels the drilling equipment technology.

First well, drilled in 2008-2009, ended in a molten rock at 2100 m depth, with a temperature of 900-1000 °C. Despite some difficulties, they controlled the well and pumped cold water into the hole to increase the permeability by breaking up the rock that is next to the magma in order to create a connection to the colder overlying geothermal environments. After setting steel casing down to the bottom of the hole, they 'allowed the hole to blow superheated, high pressure steam for months at temperatures over 450 °C'. According to the measured output, the available power was stated as sufficient to generate up to 36 megawatts electricity [25]. IDDP-1 showed that a high-enthalpy geothermal system can be created as a Magma-Enhanced Geothermal System.

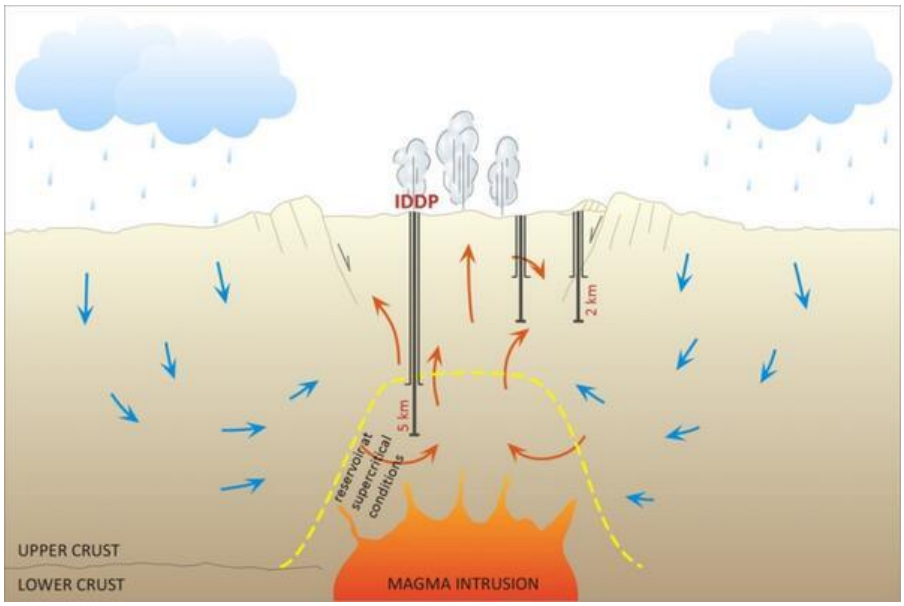

Figure 5: Illustration of Icelandic Deep Drilling Project [26].

In **Hot Dry Rock (HDR) systems**, which is the main focus of that study, there is no fluid to store or to transport the heat. The temperature in HDR systems is generally less than 650 °C [27]. The heat is stored in hot and poorly permeable rocks. They are illustrated as hot granite body in Figure 6. Main geological setting of HDR systems is the 'young intrusive bodies within 10 km of Earth's surface' [27].

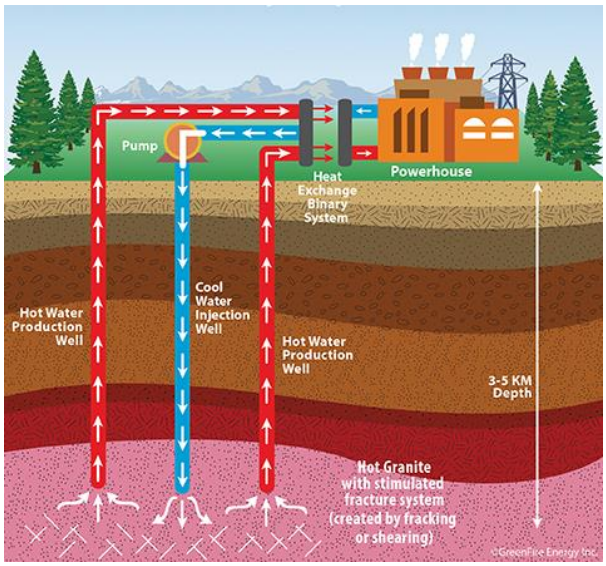

Figure 6: Illustration of an Enhanced Geothermal System [28].

Based on the heat source, HDR systems can be classified into three groups: 'igneous related, upper mantle related and local where heat is due to high concentration of radioactive minerals or large scale faulting and or fracturing'. This makes the 'recent volcanism, high-heat flow and localized radiometric heat sources' best places to look for these systems [27].

The heat mining process is achieved through hydraulic fracturing in HDR systems. The working principle is illustrated simply in Figure 6. Through a pump, cool water is injected to the hot granite body which is formerly fractured by fracking or shearing. Then hot water is produced though production wells that have an average of 3-5 km depth. Heat exchange binary system utilizes the heat and it is converted to electricity in the powerhouse.

In hot dry rock systems, understanding the tectonic setting of the target field such as stress regime is very important. Another factor that affects the site selection process of HDR projects is the water availability in the field. There should be no scarcity of water where a potential HDR project is addressed as the injected water will be the way of heat convection.

In Turkey, especially in the Aegean region, intrusive magma or recently solidified bodies are generally the source of geothermal heat. Extensive Miocene to Quaternary lava and pyroclastic occurrences are the evidences of these intrusions at the depths of Earth. Figure 7 shows the volcanic regions (colored as pink in colored print-outs) in Turkey.

Figure 7: Map of volcanic regions, colored as pink in electronic copies, in Turkey [30].

The heat flow map of Turkey is given in Figure 8. Heat flow is in units of mW/m^2. Red colored regions represent areas with high heat flow whereas blue colored regions represent sites with low heat flow (available in colored copies). High heat flow may be due to thinning of Earth crust, recent volcanism and radioactive decay. It reveals the relationship between Figure 7 and Figure 8.

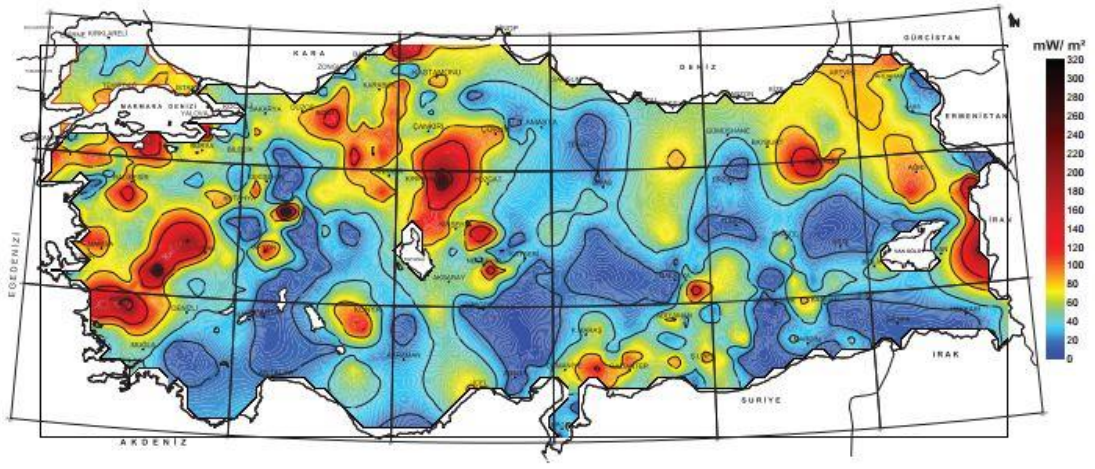

Figure 8: Heat flow map of Turkey [31].

HDR systems are great potential to increase the share of geothermal in Turkey's energy mix. General Directorate of Mineral Research and Exploration (MTA) has started to carry out

exploration of HDR systems mainly in Anatolia where young volcanoes exist. Mapping studies are completed whereas geochemical and geophysical studies are still continuing. Burçak, 2015 classifies regions with high geothermal gradient to be potential addresses for EGS applications with the expected temperature ranges as follows:

1) Geothermal regions with partial melting and anataxis/migmatite occurring in Western Anatolia in neo tectonic stage (expected temperature range at 5000 m: 450-500 °C).

2) Tertiary aged granites with subduction origin (expected temperature at 5000 m: 350 °C).

3) Geothermal resources related to buried lavas and intrusive igneous rocks in Western Anatolia and Southern Marmara (expected temperature at 5000 m: 325 °C).

4) Geothermal regions with young volcanic activities in Middle and Eastern Anatolia (expected temperature at 5000 m: 375 °C) [32].

Target fields are namely; Nemrut, Alaşehir-Kavaklıdere, Kızılcahamam, Nevşehir-Acıgöl, Aksaray, Konya-Ilgın, Kütahya-Şaphane and Çanakkale [33]. In addition to these locations, SDS Energy initiated an EGS pilot project in İzmir-Dikili region in 2010. This project aims to generate power from hydraulically fractured Kozak pluton in the region [29]. The geological characteristics, hydrogeological outlook and the tectonic setting of Dikili geothermal field are discussed in detail in Chapter 2.3.

2.2. Production and Utilization History of Geothermal Resources

The utilization ways of geothermal resources heavily depend on temperature. High temperature resources are best suited for indirect use, i.e. electricity generation, whereas low to moderate temperature resources are being used for direct purposes such as district heating, greenhouse heating, heat pumps, agricultural drying, heating of road and side-walks in winter.

Nevertheless, developing technology is now changing the temperature boundaries of geothermal sources to generate power. Further it erases the necessity of having water or sufficient permeability in reservoirs. Different thermodynamic cycles (such as Kalina or Organic Rankine Cycle) and hybridization concept as supporting geothermal with another energy source are the ways to lower the needed geo-source temperature. For the geothermal sites where heat is sufficient but permeability or fluid is once considered lacking, EGS may be deployed. The aim of EGS is to extend geothermal resources across a wide spread of geography by creating conditions that render the system hydrothermal in an economical way.

EGS covers all the sites lacking one of the key parameters for a sufficient production whereas HDR is the geothermal system only lacking fluid and permeability.

2.2.1. Indirect Utilization

Although hot water resources have been utilized as spas for centuries, even give names to locations where they exist, the use of that heat for power production began with Larderello in Italy in 1904 [34]. Power generation is a more challenging use of geothermal energy. To convert heat to electricity requires a creative engineering design process depending on the nature of geothermal resource. That 'state-gate' process yields in the most 'all-purpose' form of energy. There are three main types of geothermal power plants: Flash steam, dry steam and binary to convert geo-heat into electricity. In all those systems, the system efficiency depends on the efficiency of the all components such as heat exchanger, condenser, turbine and generator.

In dry steam power plants, reservoir produces only high temperature steam and that steam is supplied directly to the turbine as seen in Figure 9. Waste steam is sent to condenser. When it condensates, water can be utilized for heating purposes, as stated in the figure as direct heat users. Waste water is then reinjected through injection wells. The thermal efficiency of these plants is up to 20%. They produce 24% of produced geothermal energy (in GWh) in the world [13]. In Turkey, there is no example of dry steam power plants. In the world, Larderello-Italy (the oldest) and Geysers-California (the largest) are the examples of this technology.

In flash steam systems, geothermal fluid is pumped under high pressure into a separator causing some of the fluid to vaporize i.e. flash due to rapid pressure change. Then steam is separated from hot water and sent to turbine as seen in Figure 10. Remaining liquid is either sent to another tank to flash for more energy if possible or reinjected to ground. Thermal efficiency of these plants is 10-20%. These systems provide the 63% of produced geothermal energy in the world [13]. In Turkey, Germencik (double flash, Figure 11) and Kızıldere (single flash) plants are the examples of this technology.

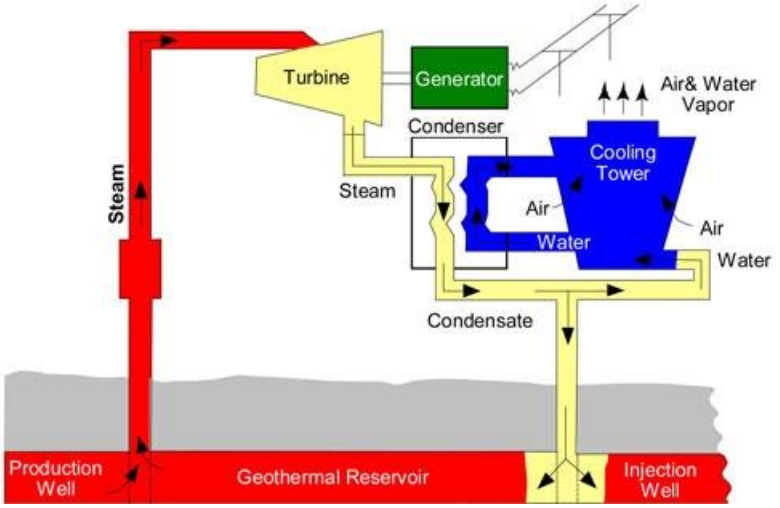

Figure 9: Illustration of Dry Steam Power Plants [35].

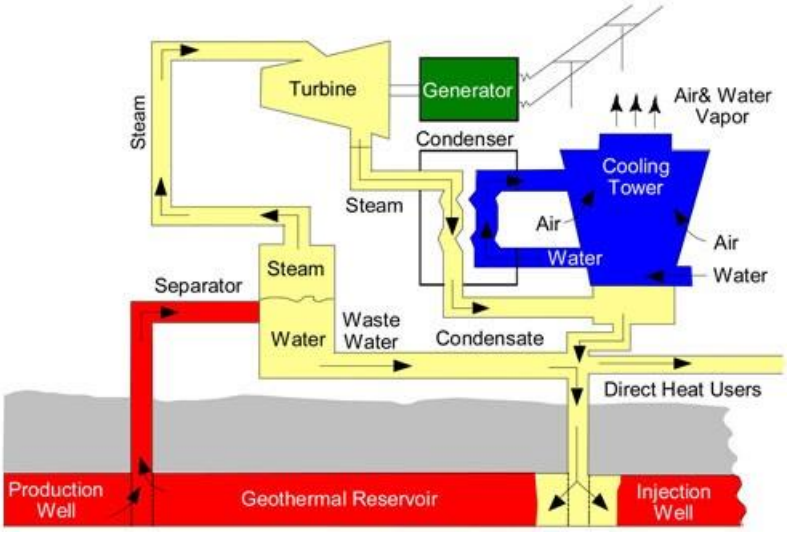

Figure 10: Illustration of Flash Steam Power Plants [35].

Figure 11: Photo of Germencik Geothermal Power Plant in Turkey (double flash technology with installed capacity of 47.4 MW_e) [36].

In binary cycle power plants, geothermal fluid is used just to boil a working fluid which has a lower boiling point and higher molecular weight than geo-fluid. After being utilized, geo-fluid is reinjected into the ground to maintain the reservoir life time. There are different thermodynamic cycles used in binary power plants. One of them is Kalina Cycle which uses a working fluid with at least two components, generally water-ammonia. Another most common cycle is Organic Rankine Cycle (ORC), which generally employs butane, propane, pentane and their iso- versions as working fluid. Figure 12 illustrates a schematic diagram showing the basic concept of a low-temperature geothermal binary ORC system for electrical power generation. Binary cycle power plants have a thermal efficiency of 10% [11]. The attractive side of these systems is to make possible economic production of electricity from geothermal resources having temperature less than 150 ºC.

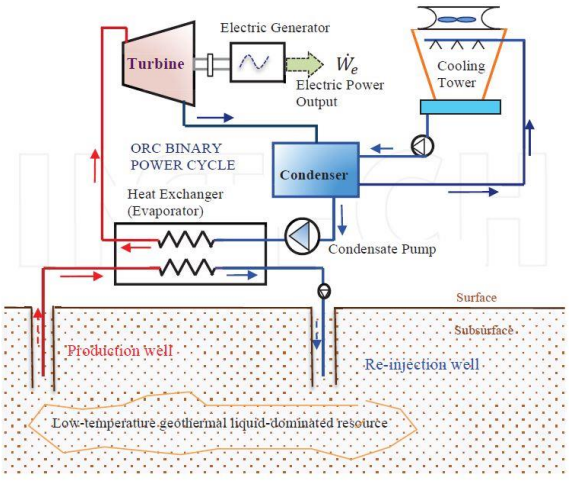

Figure 12: Schematic diagram showing a low-temperature geothermal binary ORC system for electricity generation [37].

Low temperature power cycles are relatively new in industrial scale. Thus reference knowledge is limited. Since it is a hot research area, theoretical understanding of low temperature power cycles is increasing. Although field data is kept confidential, so is limited, practical utilization of this knowledge is also increasing. In Turkey, Tuzla (shown in Figure 13), Dora-1 and Kızıldere-Binary geothermal plants are the examples of binary cycle power plants.

Figure 13: Photo of Tuzla Geothermal Power Plant in Turkey (with installed capacity of 7.5 MW_e -Binary cycle) [38].

2.2.2. Direct Utilization

The heat of geothermal sources with low to medium temperature is directly used for balneology, space heating, greenhouse heating, agribusiness and heat pump applications. Based on the real statistics provided by Mertoğlu et al., (2015) 90,000 apartment residences are heated by geothermal in 16 cities of Turkey [39]. Here one residence equivalence is assumed to be 100 m^2 floor area [64]. The main component of geothermal heating systems is heat exchanger and its efficiency is generally accepted as the system efficiency for simplicity. Because it is based on the efficiency of transferring heat energy from geo-fluid to a secondary fluid. A schematic illustration of a geothermal district heating system is given in Figure 14. Here, geo-fluid (colored as gray) transfers its heat to working fluid (colored as green) in the heat exchanger. Geo-fluid is then reinjected to the subsurface and working fluid circulates through the district heating system.

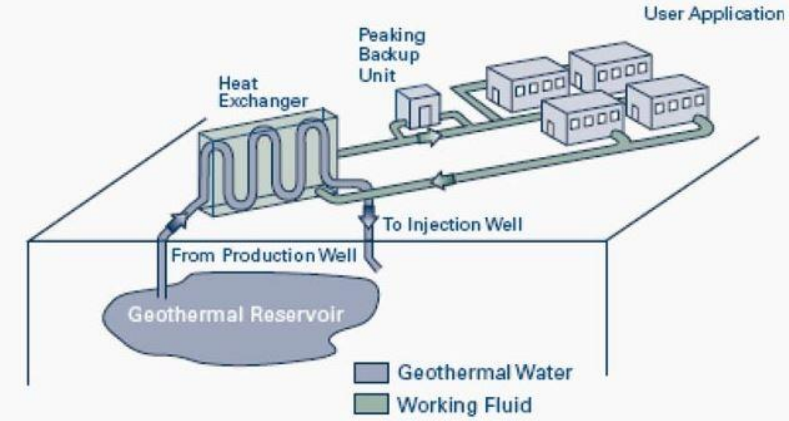

Figure 14: An example of geothermal district heating systems [40].

2.3. Dikili Geothermal Field

The latitude is 38º91´N and longitude is 26º55´E for Dikili county town center. However, the study area involves not only Dikili but also a larger area surrounded by Bergama in the south, Dikili and Ayvalık in the west coast, Madra Mountain in the north. Madra Mountain is located 100 km to the North of Izmir and hosts archaeological Bergama site in the Southern slope of the mountain. The study area involves about 20 hot springs, shown as blue circles in electronic copies, in Figure 15. On the left hand side of the figure, Dikili area is seen as a red rectangular positioned to the north of main geological sites, marked as yellow, in Western Anatolia. On the right hand side, study area is seen in detail as a double chin surrounded by hot springs, colored as blue circles.

Figure 15: Location map of Dikili-İzmir.

In Dikili, the climate is semiarid with an annual precipitation of 652 mm and the annual average temperature is 16.5 ºC [41]. Mean monthly temperature values are shown in Figure 16. Based on that information, heating is needed for six months in Dikili considering the months with a temperature below 18 ºC.

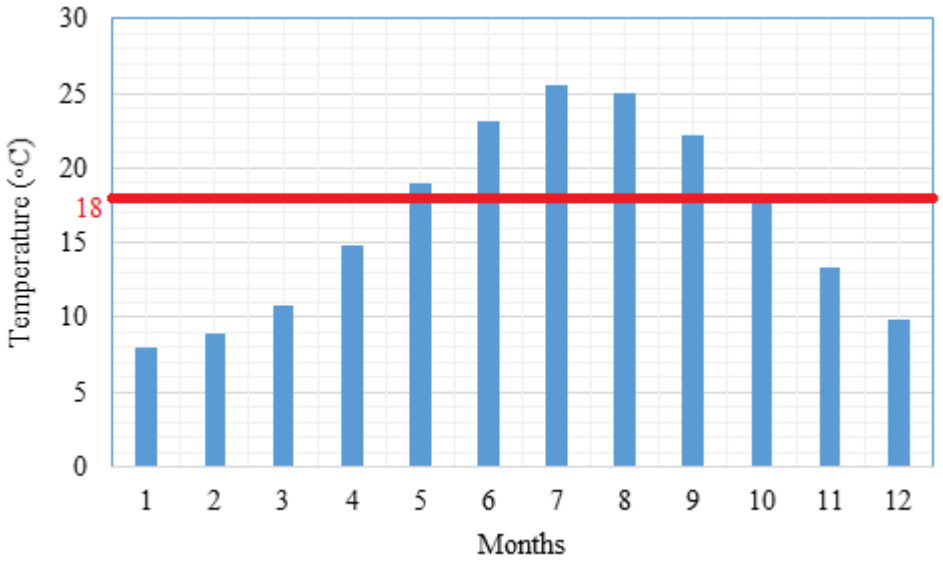

Figure 16: Mean monthly temperature values in Dikili, modified from [41].

The average annual solar irradiance is 3.97 kWh/(m^2day) and the hours of sunshine is 8.09 h/day [42]. Total solar radiation of study area is 1400-1550 kWh/m^2/year. These values do not meet the minimum requirements (total solar radiation>1650 kWh/m^2/year) for any kind of solar plants as stated in GEPA, 2010 [42]. That is why supporting geothermal with thermal solar power is not an option to increase the enthalpy of Dikili geothermal resources [43].

Identified geothermal systems in Dikili-Bergama area are all hydrothermal systems surrounding the Madra Mountain as seen in Figure 15. Northeast-Southwest trending ellipsoidal granitic Kozak Pluton, forming 500 to 800-meter-high (highest point 1,341 m) mountains surrounded by Yuntdağ Volcanites at lower elevations, may be a hot dry rock system. This study is concerned with the comparison of direct or indirect utilization of hydrothermal (Yuntdağ Volcanites as reservoir rock) and enhanced geothermal systems (Kozak pluton as reservoir rock) in the region.

2.3.1. Geological Outlook

Previous studies [29, 44, 45] defined eight formations in the study area: Çamoba, Kınık, Kozak Granodiorite, Ballıca, Soma, Yuntdağ Volcanites, Rahmanlar Agglomerate and Dededağ Basalt from oldest to youngest. All formations are overlied by Quaternary alluvium at the top. Geological map of the area is given in Figure 17.

Elevation contours are drawn for each 100 m. They get close to each other in Madra Mountain representing higher elevation of the mountain compared to its vicinity.

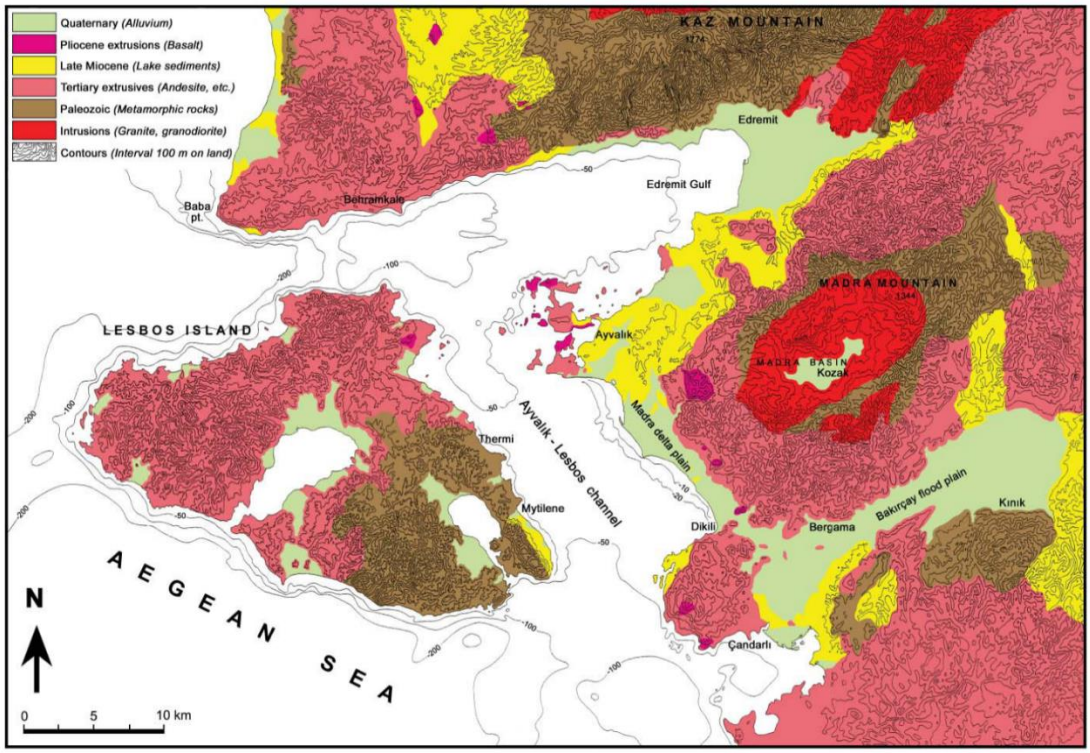

Figure 17: Geological map of the study area with elevation contours [48].

Permian aged Çamoba formation, which is the oldest unit in the study area, is composed of sandstone, siltstone and limestone. Its expected average thickness is around 250 m. Mesozoic Kınık formation is composed of conglomerate, sandstone, siltstone, mudstone, clayey limestone and limestone. Its average thickness is 400 m [44]. Altunkaynak and Yılmaz, 1999 state that during the long history of ascent of Kozak pluton, a variety of emplacement mechanisms occured at different depths since 'Kozak pluton exhibits different effects on the host rocks along different contacts'. The Kozak pluton is mainly composed of granodiorite [49]. Although its thickness is not known (it may go deeper under Çamoba and Kınık formations), an average thickness is given as 800 m [44]. Özen et al. (2005) states that Yuntdağ volcanites unconformably overlie Kınık formation and are classified into three groups:

Yuntdağ volcanites-I, which is the oldest part of the Yuntdağ formation, consists of widely altered andesite. Yuntdağ volcanites-II consists of dark compact basalt, pyroxene andesite and hornblende andesite. The youngest part of Yuntdağ formation is Yuntdağ volcanites-III [45]. It consists of rhyolite, hornblende, biotite andesite and dacite [29]. The thickness of Yuntdağ formation is 400 m [44]. Upper Miocene Soma formation consists of alternation of siltstone, marl, conglomerate, sandstone and clayey limestone. Its thickness is 1000 (?) m. Pliocene Rahmanlar formation is mainly composed of agglomerate. Its thickness is 400 m. Pliocene Dedebağ formation overlies Rahmanlar formation. Dedebağ formation mainly consists of basalts. Formation thickness is 100 m. All the units are overlied by Quaternary alluvium at the top. Its thickness is 100-150 m. Figure 18 illustrates these formation characteristics with a generalized stratigraphic columnar succession below.

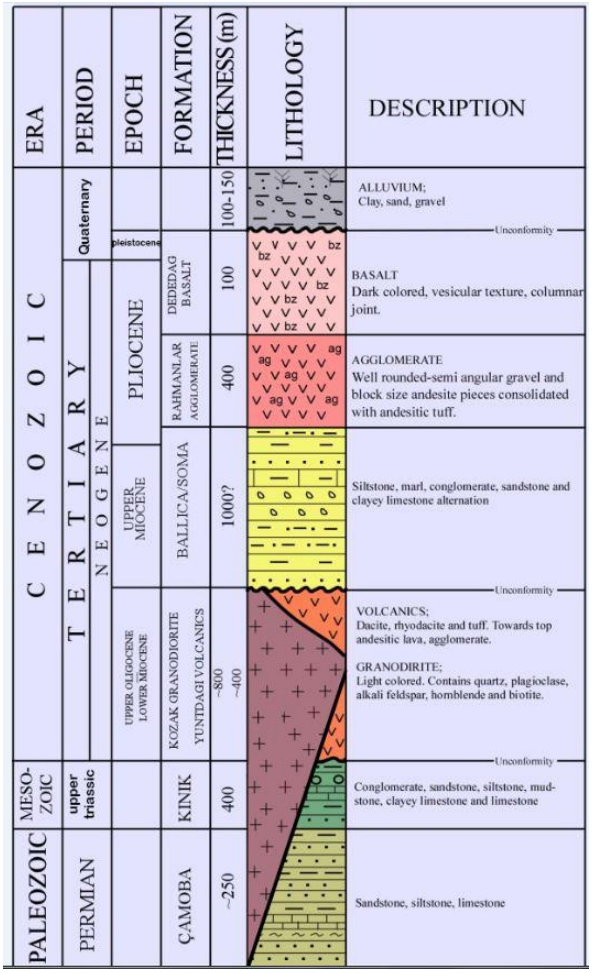

Figure 18: Generalized columnar section of study area, modified from [44].

Among aforementioned eight formations, Yuntdağ Volcanites behave like reservoir rock with its highly fractured structure due to tectonism and its hydrothermal alterations. Generally cap

rock is not seen in study area. However, at some locations, Soma formation and the thick tuff and marl layers within the Yuntdağ formation behave like cap rock.

The heat source in the region has been a subject of debate. Source of the heat stored within the Earth crust could be heat coming from core, subsurface magma intrusions or plutonic rocks formed from: magma at 10-20 kilometers of depth, young volcanic rocks such as hot lava or pyroclastic rocks reaching to surface, radioactive decay of U, Th and K radioactive isotopes that are abundantly occurring in some igneous rocks, excess amount of friction along faults and fractures in tectonic belts and local exothermal reactions in permeable formations. Hou et al. (2015) suggested that radioactive decay in Kozak Granodiorite is the heat source in the region [29], whereas Özen et al. (2008) claimed that shallow magma is the heat source since Kozak pluton is too old to be [46]. In the final report of Japan International Cooperation Agency on 'The Dikili-Bergama Geothermal Development Project', the heat source is stated as deriving from both tectonism and volcanism due to the fact that the volcanic activity and tectonic movements are very intense in the study area [47].

Figure 19 shows crustal structure and magmatic intrusions in an extensional tectonic environment. Plutonic intrusions in the subsurface could be the source of local anomalies shown in heat flow maps as thin continental crust and plutonic intrusions jointly are responsible for high geothermal heat.

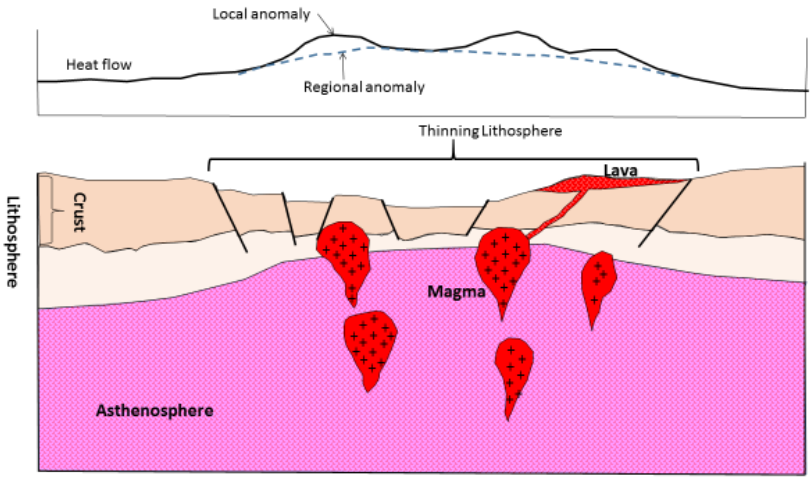

Figure 19: Schematic model of thin Earth Crust and plutonic intrusions developed to explain high heat flow and associated thermal resources in the study area.

2.3.2. Tectonic Setting

The western Anatolia is accepted as one of the world's most rapidly-extending, crustal thinning zones with an extension rate of 14 ± 5 mm/year [50]. Dikili district is a tectonically active area, where this N-S extensional regime, causing E-W extending grabens, exist.

Kozak Granite forming Madra Mountain is surrounded by Yuntdağ volcanites at its foothills and all geothermal springs are associated with Yuntdag volcanites around the Madra Mountain. The distribution of these hot springs is controlled by fracture patterns. Dominant fractures in Kozak Pluton (from image lineaments) are marked in red and active graben faults are shown in black lines in Figure 20.

Figure 20: Dominant fractures in Kozak Pluton from image lineaments (marked in red) and active graben faults (shown in black lines) affecting the occurrences of hot springs (marked as blue circles in colored copies).

Based on the available information related to study area and our observations, it is concluded that water seeping into deep seated dominantly northeast-southwest trending fractures in Kozak granite is heated at depth. These fractures are intersected by active normal graben faults which form a pathway for heated water to flow out towards surface. Water table elevation in Kozak fractures is higher than the elevations of graben fault traces on the surface. This builds a hydrostatic pressure for water to form hot springs on the surface.

In the Aegean Region, hot-spring and drilling sites are in normal fault zones separating horst and graben structures. These normal faults are acting as discharge pathways for hot water. Intake fractures which enable seepage of water down in the horst areas are different than discharge fractures in terms of their origin and fracture geometries. The flow-process of a geothermal spring is closely interrelated with the geometry of intersection line between intake and discharge fractures. Figure 21 illustrates fracture patterns and geomorphological factors in flow mechanism of hot springs.

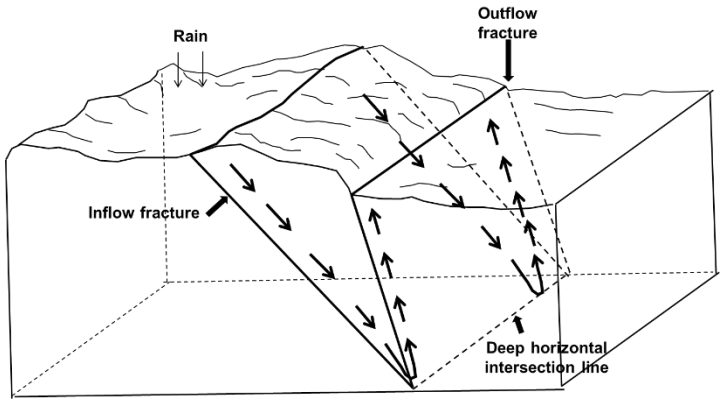

Figure 21: Schematic illustration of fracture and geomorphological factors in flow mechanism of hot springs.

Generally, geothermal springs are at topographically low elevations around a mountain. Majority of geothermal drilling is also located in these areas to find artesian water coming to surface without pumping. In the Aegean Region, hot-spring and drilling sites are in normal fault zones separating horst and graben structures. These normal faults are acting as discharge pathways for hot water. Intake fractures which enable seepage of water down in the horst areas are different than discharge fractures in terms of their origin and fracture geometries. The flow-process of a geothermal spring is closely interrelated with the geometry of intersection line between intake and discharge fractures. Several fracture or fault intersection models are possible as follows:

- **Oblique strikes of outflow and inflow fractures, causing an inclining intersection**: If strikes of two fractures are not parallel, intersection line between two plains will be inclined as illustrated in Figure 22. As a result, two fractures will be crossing each other at gradually changing depths based on the inclination angle. Hot water springs aligned on the outflow fracture will show increasing temperature in the inclination direction.

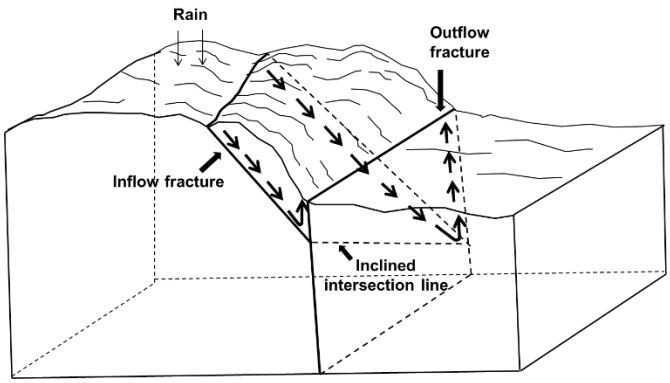

Figure 22: Oblique strikes of outflow and inflow fractures cause an inclining intersection line.

- **Outflow fracture intersecting multiple inflow fractures:** In this case, hot water rising up to surface will be coming from different depths as seen in Figure 23. The temperature of the hot water obtained will be an average based on mixing principles.

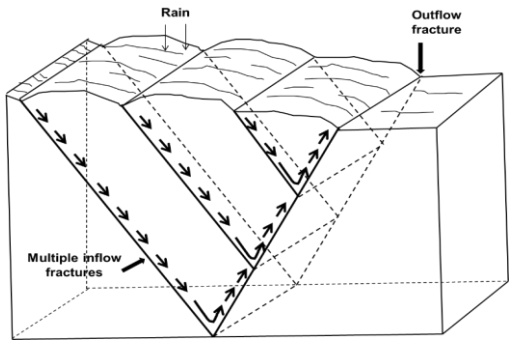

Figure 23: Outflow fracture intersecting multiple inflow fractures.

- **Multidirectional fractured rocks:** Sometimes a geological formation is crossed by multiple fracture systems of different directions as seen in Figure 24. In this case, the formation will have a good fraction of fracture porosity. If the geomorphological conditions are appropriate for hydrostatic head pressure, these fractures will form pathways for ground water to flow. In this model, cold and hot waters will be mixing therefore high temperature will not be obtained from these springs. However, if deeper wells are drilled, hot water might be obtained.

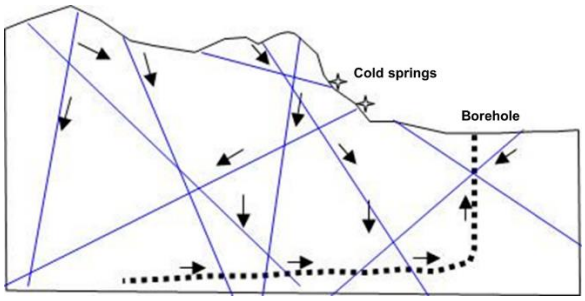

Figure 24: Multidirectional fractured rocks.

- **Intersecting fractures in a flat terrain:** Although a high geothermal gradient and appropriately intersecting fractures in a rather smooth terrain, no flow occurs and no geothermal spring is observed. The reason is the lack of hydrostatic pressure which is needed as a drive for the water to flow (Figure 25). In such an area, both intersecting fracture systems function as an intake fracture and hot water does not flow upwards. Flat topography is not appropriate for geothermal hot spring manifestation, but intersecting fractures by a horizontal well might be considered in hot-dry rock projects. These resources are existing in subsurface and are still viable resources, known as 'blind resources' that cannot be seen at the surface.

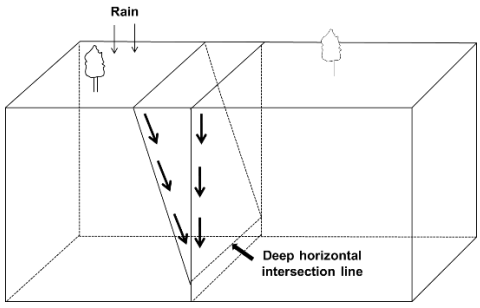

Figure 25: Intersecting fractures in a flat terrain.

- **Fractures of parallel strikes but opposite dipping fracture intersecting at shallow or deep depths:** This type fractures reveal a horizontal intersection. When dips are in reverse directions intersection is most likely at a shallow depth, however, this depends on the dipping angles of inflow and outflow fracture planes (Figure 26). Spring water temperature is low if intersection occurs at a shallow depth.

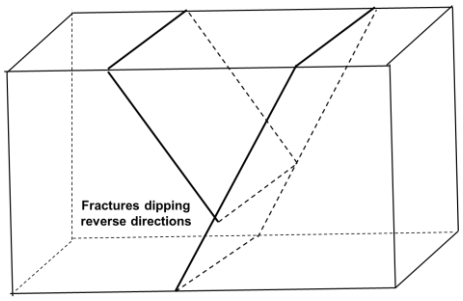

Figure 26: Fractures of parallel strikes but opposite dipping fracture might intersect at shallow or deep depths.

- **Shallow intersecting parallel strike fractures creating geothermal springs:** This is similar to the deep intersecting fractures but here fractures are intersecting at a shallow depth because of low dipping angles of fractures. The lower the dipping angle the shallower the intersection line is obtained. Consequently, spring water temperature is not very high in this case as illustrated in Figure 27**.**

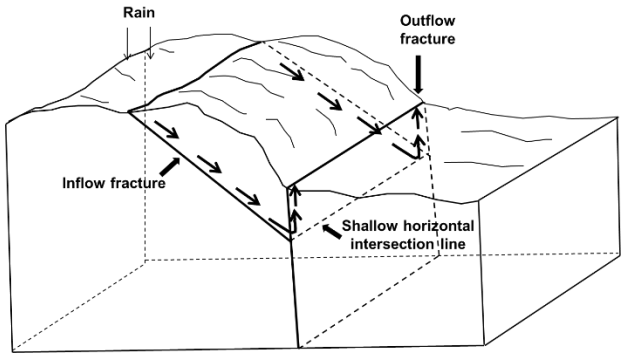

Figure 27: Shallow intersecting parallel strike fractures might create geothermal springs but water temperature might not be very high.

- **Intersection of unparalleled fracture planes:** When strikes of two fracture planes are not parallel, intersection line will not be horizontal. If both planes are vertical, intersection line will be a vertical line (Figure 28a). If one of the fracture plane or both are dipping the intersection line will be an inclined line (Figure 28b). Vertical or inclined intersection lines may form a spring of mixing waters at different depths. This type of intersection generally is not very favorable as a geothermal energy resource. Vertical and inclined intersection lines are venues of mixing hot and cold waters rising upward and are not favorable for hot springs.

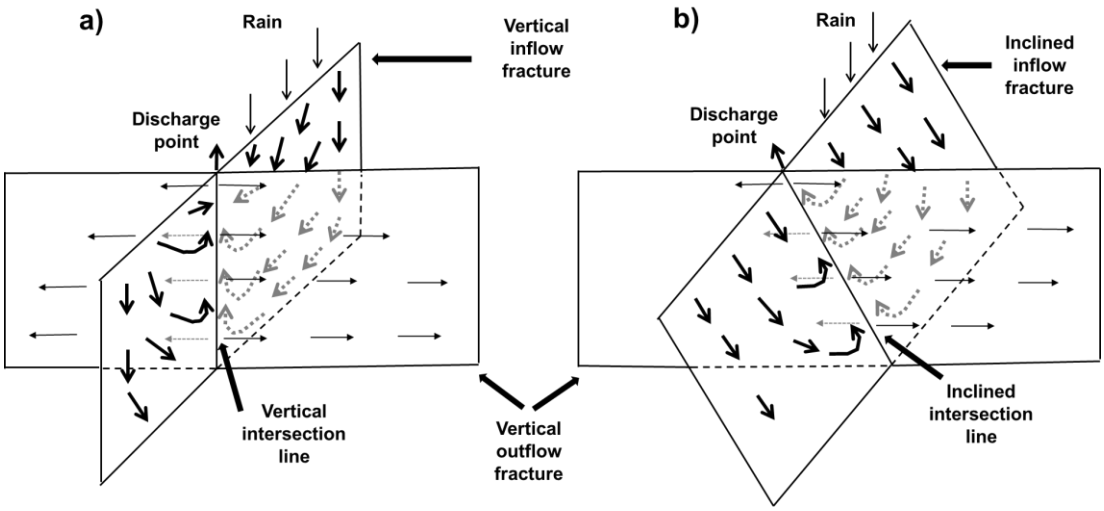

Figure 28: Intersection of unparalleled fracture planes: (a) vertical planes reveal a vertical intersection line, (b) if one or both planes are dipping with an angle intersection line is inclined.

- **Non-intersecting parallel fracture planes:** As aforementioned, occurrence of a geothermal spring requires appropriately intersecting two fractures, one intake fracture providing pathway for water to flow downward and one discharging (outlet) fracture providing pathway for water to flow upward to the surface. A single fracture system of parallel planes cannot initiate hot water springs even though a high geothermal gradient exists in the area. Hot water production might be possible if parallel fracture system is intersected by a deep deviated or horizontal borehole (Figure 29).

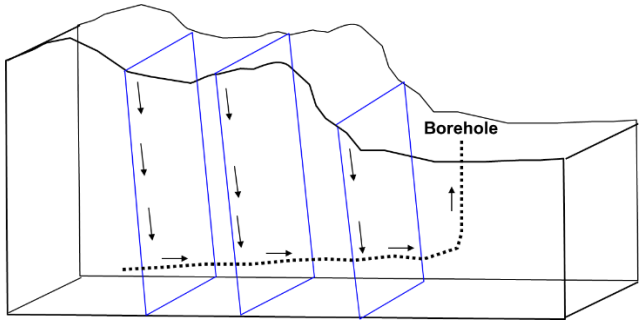

Figure 29: Non-intersecting parallel fracture planes do not create geothermal springs, but could be potential if crossed by deep directional boreholes.

2.3.3. Hydrogeological Outlook

Dikili has number of hot springs with changing temperature from 30 to 100 ºC [51]. The hydrogeological studies indicate a minimum age of 50 years in subsurface based on radioactive isotope chemistry. Stable isotope analysis show that thermal waters are of meteoric origins, which recharged in Kozak region, heated at depth and moved up to the surface along the faults [45].

The types of thermal waters are Na-HCO_3-SO_4 in Dikili, Na-SO_4-HCO_3 in Kaynarca and Na-Ca-SO_4 in Kocaoba [45]. Dissolved salts, SO_4^{-} and HCO_3^{-} content of thermal waters are related to their depths. SO_4^{-} is dominant for thermal waters coming from depths of 500-700 m whereas HCO_3^{-} is dominant for thermal waters coming from 700 m depth. Thus it is concluded that the reservoirs of the thermal waters in the study area are not very deep because of the low SO_4^{-} and HCO_3^{-} values. High values of Cl^{-} ion in Bademli spring are due to the sea water mixing. Based on this information, Tabar et al. (2013) stated that the temperature of the thermal waters in Dikili geothermal area is not high [51].

Thermal waters in the study area are slightly acidic which may be due to the contact with carbonate rocks [52]. According to the mineral equilibrium modelling, calcite, aragonite and dolomite scaling problems are expected in production wells [45].

2.3.4. Drilling and Production History

Dikili geothermal field has been the focus of direct utilization ways such as district heating, greenhouse heating and thermal tourism since early 2000's. Although the geothermal investigations had started in the region after the big earthquake in 1939 [53]. Nowadays there are more than 30 wells in the field with well temperatures ranging from 41.5 to 131.4 °C. Some of them are listed in Table 6. As of 2015, 1160 residences (one residence is assumed to have 100 m^2 floor area) and 1,000,000 m^2 greenhouses are being geothermally heated in the region [14].

Table 6: Wells in Dikili Geothermal Field (abbreviations are WB: well bottom, WI: inside the well, WH: well head, A: artesian, C: compressor, P: with pump).

Well Name	Ownership	Well Depth (m)	Well T (◦C)	T Measurement Place	Flow Rate (l/sec)	Flow Rate Measurement Way	Reference
K-1	MTA	1500	130	WB	-		(Karahan. n.d.)
B-1	Dikili Belediyesi	33.5	119.3	WI	48	A	
B-2	Dikili Belediyesi	36	98	WH	30	A	
B-3	Dikili Belediyesi	26.80	120	WB	34.8	A	
T-1	İzmir İl Özel İdaresi	355	130.7	WB	42	A	
T-2	İzmir İl Özel İdaresi	356	131.4	WB	47	A	
T-3	İzmir İl Özel İdaresi	547	97	WH	45	C	
A-0	Agrobay Seracılık	256	98	WH	40	P	
A-1	Agrobay Seracılık	208	93	WH	30	P	
A-2	Agrobay Seracılık	254	97.7	WH	15	P	
A-3	Agrobay Seracılık	392	110	WI	50	P	
A-4	Agrobay Seracılık	420	110	WI	50	P	
Z-1	Zeytindalı Termal	254	45	WH	5	A	
Ç-1	Vegevital-Çakır Eğitim	210	110	WI	30	C	
Ce-1	Ali Celep	253	105	WI	40	C	
İDB-1	MTA	1400	50	-	1	C	İzmir ili yenilenebilir enerji sektör analizi (Nisan 2012)
İDB-2	MTA	1500	69	-	55	C	
İDH-2010/11	MTA	1250	145	WB	4	A	
İDH-2010/11	MTA	1250	71.5	WH	38	C	
İDK-2010/13	MTA	270.6	47.5	-	35	C	
İDD-2010/17	MTA	572	51.5	-	50	C	
İDN-2011/1	MTA	583	74.9	-	65	C	
DKO-1(2007)	MTA	729.5	41.5		9	P	
WB: WELL BOTTOM			A: Artesian				
WH: WELL HEAD			P: with Pump				
WI: INSIDE THE WELL			C: with Compressor				

CHAPTER 3

METHODOLOGY

The objective of the present study is to perform a feasibility study for an enhanced geothermal system application in Dikili-İzmir region. This feasibility study is composed of three main parts that are geothermal resource assessment, impact analysis and critical analysis. Since earth sciences deal with subsurface that yields in uncertainty in related parameters, geothermal resource assessment is done by employing probabilistic methods rather than deterministic ones. Among the other resource assessment methods, the volumetric method is selected to calculate the stored heat energy since it is well suited to being adapted to a probabilistic approach. To apply this method, Monte Carlo Simulation technique is employed to allow the variables to vary over a defined range, by minimum, maximum, and/or most likely values, with a defined probability distribution. While using this technique, a random number is first generated and then it is used to determine the values of the variables within the defined probability distribution. The stored heat is then calculated using the generated values. This process is repeated until a well-defined probability distribution is observed as the expectation curve (i.e. a plot that shows the distribution of possible outcomes under uncertainty) for heat output (MW_t or MW_e) is obtained. Sensitivity of the output to the number of simulations is also tested. In the second part, an impact analysis that reveals the heavy hitters among all the input parameters is done by plotting tornado charts. In the third part, a critical analysis is done to highlight the sustainability attributes of the discussed systems. The summary of the workflow is illustrated in Figure 30.

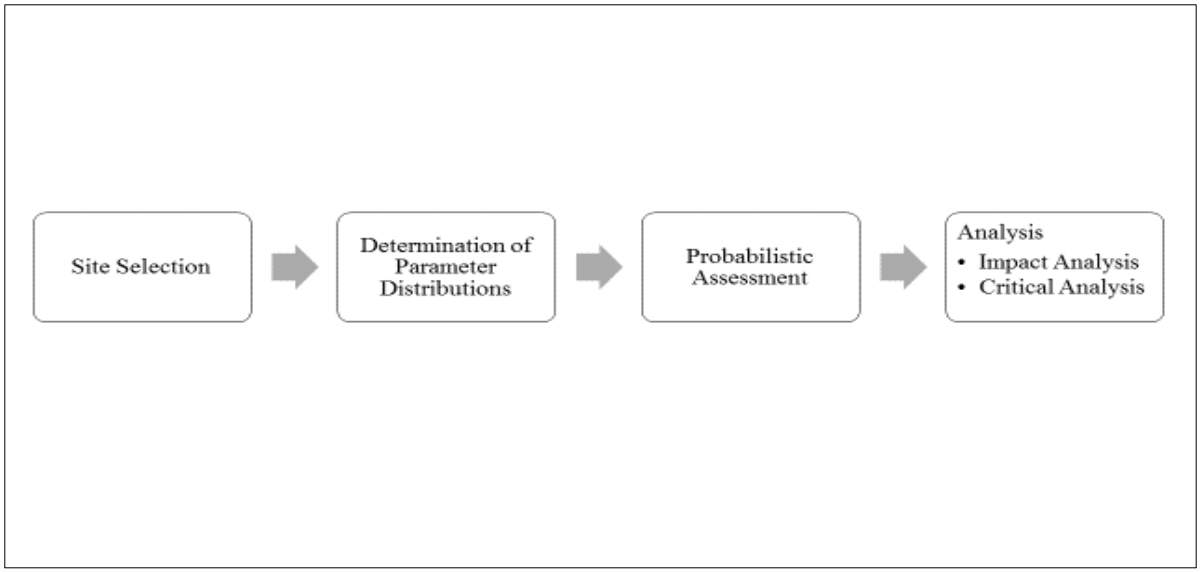

Figure 30: Workflow of methodology.

3.1. Geothermal Resource Assessment

Muffler and Cataldi (1978) defines geothermal resource base as 'all the thermal energy in the earth's crust under a given area, measured from mean annual temperature' [54]. There are four main methods used in geothermal resource assessment:

1. **Volume method**: In this method, heat energy stored in the reservoir is equal to the sum of heat stored in certain volume of rock (solid part) and water (fluid part) considering the fluid in the hydrothermal reservoir is only water, not with steam.
2. **Surface thermal flux method:** It calculates the thermal energy that is transferred conductively from the soil to the atmosphere and to the surface waters in a given unit of time.
3. **Planar fracture method:** Heat is transferred first to the fracture by conduction and then along the fracture by convection.
4. **Magmatic heat budget method:** This method considers an estimate of the number, size, position and age of young igneous intrusions in addition to their cooling history. It is valid only in volcanic regions.

Muffler and Cataldi (1978) suggested that among these four methods, volume method is the most useful one for accessible resource base calculations. All the equations employed in this method are as follows [54]:

$$Q_t=Q_s+Q_w, \quad (3.1)$$

where;

Q_t: total heat content, kJ

Q_s: heat content in solid, kJ

Q_w: heat content in water, kJ

$$Q_t = (1-\phi)\ c\ \rho\ (A*h)\ T_u + \phi\ c\ \rho\ (A*h)\ T_u, \quad (3.2)$$

where;

Q_t= Heat energy, kJ

ϕ = Porosity, fraction

c= Specific heat capacity, kJ/kg-^oC

ρ= Density, kg/m^3

A= Area of the reservoir, m^2

h= Reservoir thickness, m

T_u= Utilization temperature, ^oC

and subscripts t, s and w stand for total, solid rock and water, respectively.

$$RHE = (Q_t*RF)/(t*LF), \quad (3.3)$$

where;

RHE: recoverable heat energy, kJ

RF: recovery factor, fraction

t: project life, seconds

LF: load factor, fraction

Load factor is the ratio of total time in which the system is active in a year.

$$NEP = RHE*CF, \quad (3.4)$$

where;

NEP: net electrical power, MW_e

CF: conversion factor, fraction

Conversion factor represents the ratio that accounts for the efficiency in heat transfer and electricity generation (i.e. transduction). It mainly depends on the efficiency in heat exchangers for direct utilization ways. For indirect utilization ways, it depends on the efficiency of all system components as explained in Chapter 2.2.

3.2. Probabilistic Assessment

Uncertainty can be represented in terms of a probability range of an event's occurrences. The degree of uncertainty is introduced in the heat in place calculations by assigning a range of probabilities attached to an input parameter. A probability distribution function can be developed for an input parameter based on the frequency of occurrence of various values of that parameter. Further, cumulative distribution plots often an S-curve can be generated to show the probability of the outcome [55].

3.2.1. Statistical Distribution Functions

Probability distributions are classified mainly into two groups: Discrete and continuous. Continuous distributions are binomial, normal, triangular, log normal and uniform. In uniform distribution, minimum and maximum values are entered and all the values between them have same frequency to occur. In triangular distribution, minimum, most likely and maximum values are entered to the model [55]. In this study, MS Excel was used to perform Monte Carlo simulation. The basic steps in this process are summarized below:

- In the excel sheet, list all variables with their corresponding minimum (x_l), most likely (x_m) and maximum values (x_h).
- Calculate x_r for each variable:

$$xr = \frac{xm - xl}{xh - xl} \tag{3.5}$$

- For each variable;
    - Generate n rows of random numbers between 0 and 1 (by using =RAND() formula in Excel)
    - For each random number (r_n), calculate x_n, which will result in n values of each variable with a triangular distribution:

$$xn = \{xl + \sqrt{(xm - xl)(xh - xl)(rn)} \qquad \text{if } r_n < x_r \tag{3.6}$$

$$xn = \{xh - \sqrt{(xh - xm)(xh - xl)(1 - rn)} \qquad \text{if } r_n \geq x_r$$

- Calculate simulated parameter as a function of triangularly distributed x_n values for each of the n rows.
- Generate a histogram and cumulative expectation curve of calculated values of the simulated parameter.

To generate a histogram and cumulative expectation curve (i.e. cumulative probability plot):

- Load Data Analysis Add-In in Excel.
- Go to data tab and click on Data Analysis, select histogram and click OK.
- In the opened window;
    - Input range: select values you have calculated.
    - Bin range: leave it blank or input manually determined bin ranges.
    - Output range: any cell you would like to see the output.
    - Check 'cumulative percentage' so that cumulative probabilities are output.
    - Click OK.
- Add another column and subtract the probabilities from 1 to generate the expectation curve.
- Plot bin values vs. new probabilities and read values that correspond to 10%, 50%, 90%.

3.2.2. Input Parameters and Their Distribution Histograms

In this study, the required input parameters and the probability density functions that represent them in the model are given in Table 7. All the histograms and cumulative expectation curves presented below were plotted for electricity generation case from both reservoirs. The PDFs and CDFs are not repeated for heating case since the parameters that show distribution are common for both cases.

Table 7: Input parameters and their probability density functions (PDFs) defined in the model.

Parameter	PDF
Porosity	Triangular
Area	Triangular
Thickness	Triangular
Rock & Fluid Temperature	Triangular
Fluid Density	Triangular
Recovery Factor	Triangular
Rock Density	Uniform
Project Life	Constant
Load Factor	Constant
Conversion Factor	Constant
Specific Heat Capacity of Fluid	Constant
Specific Heat Capacity of Rock	Constant
Fluid Utilization Temperature	Constant

The following data and the assumptions are taken into consideration:

1. Porosity:

Based on the previous resource assessment studies [56, 57, 58], porosity is represented by triangular PDF in this study as seen in Figure 31. The porosity values of granodiorite given in the literature [59] are 0.01 and 0.03 assigned as minimum and maximum respectively. For Yuntdağ volcanites, since they are mainly composed of andesite, porosity values of andesite stated in the literature are chosen as minimum 0.01 and maximum 0.03 [59]. Since andesite and granodiorite are both igneous rocks, it is normal to have same porosity range up to 2 significant digits. Hou et al. (2015) estimated the porosity of Yuntdağ Volcanites as 0.0129 and of Kozak pluton as 0.02 based on field study and related literature [29]. That is why these values are assigned as most likely values in the model.

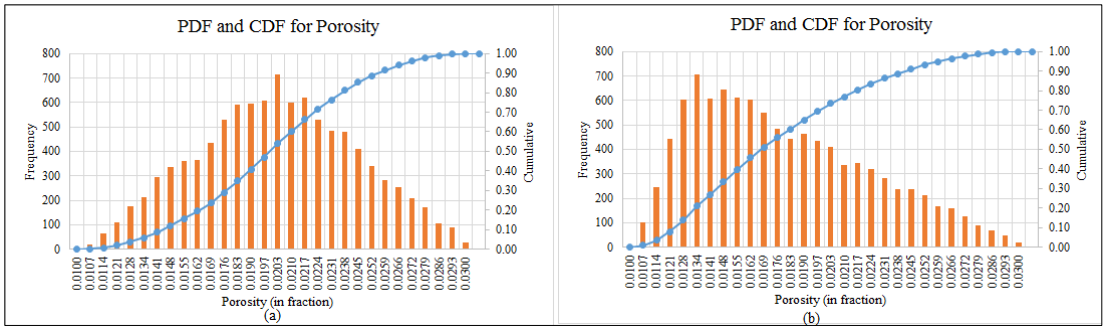

Figure 31: Histograms (as PDF) and cumulative expectation curves (as CDF) for porosity with triangular distribution: a) EGS b) Hydrothermal.

2. Area:

Area is represented by triangular PDF in this model as seen in Figure 32 based on the related previous studies [56, 57, 58, 60]. The reservoir area can be calculated exactly by the help of resistivity maps. Due to the unavailable data, for Yuntdağ Volcanites, reservoir area is taken as $1.5*10^7$ m^2, $3.0*10^7$ m^2, and $4.5*10^7$ m^2 as minimum, most likely and maximum values, respectively.

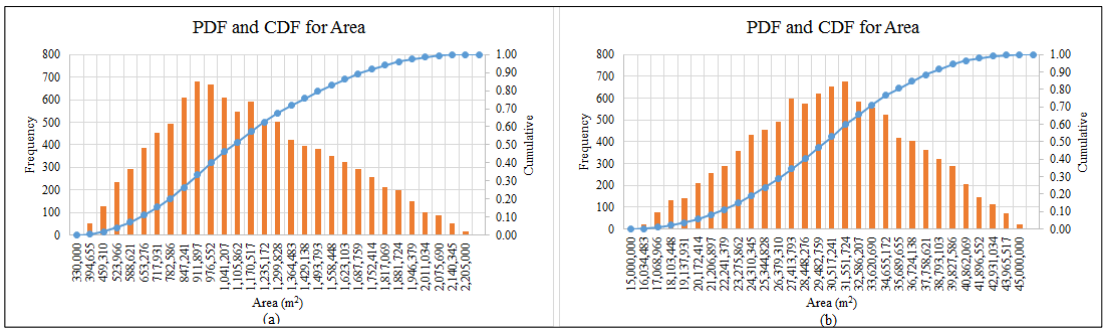

Figure 32: Histograms (as PDF) and cumulative expectation curves (as CDF) for area with triangular distribution: a) EGS b) Hydrothermal.

For Kozak-EGS, the area of the artificial reservoir is taken as $3.3*10^5$ m^2 (min.), $8.8*10^5$ m^2 (most likely), $2.21*10^6$ m^2 (max.) for Kozak granodiorite considering two horizontal wells, with a changing well length and distance between wells. A sample configuration is given in Figure 33. In the figure, two horizontal wells are seen from the top. For the minimum case, well lengths are 1000 m and they are placed apart from each other by 250 m. For the most likely case, well lengths are 1500 m and they are placed apart from each other by 500 m. For the maximum case, well lengths are 2000 m and they are placed apart from each other by 1000 m. For a more realistic representation of reservoir conditions, the effect of hydraulic fracturing has been taken into consideration. Thus the stimulated reservoir area is calculated not only as

the area between the wells but also with the increase in front and rear of wells as 25 m for each and with the increase along well direction as 100 m. In this way, new dimensions of stimulated reservoir area are (250+25+25) m and (1000+100) m for the minimum case. Similarly, for the most likely case, dimensions are (500+25+25) m and (1500+100) m. For the maximum case, dimensions are (1000+25+25) m and (2000+100) m.

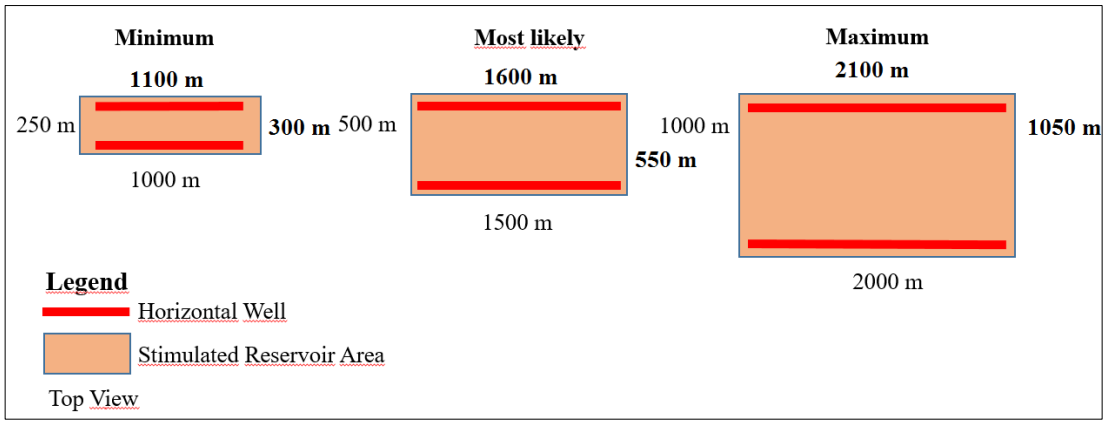

Figure 33: Sample configuration of well layout and stimulated reservoir area from the top view not to scale (bold numbers are the new dimensions and thick red lines represent horizontal wells in colored copies).

As mentioned earlier, in enhanced geothermal systems a natural reservoir does not exist due to the extremely low permeability of these systems. Thus an artificial reservoir is created by hydraulic fracturing. However, hydrothermal systems have natural reservoirs. To come up with a fair comparison between these two systems, net electrical and net thermal power were calculated also for a unit volume case when the reservoir area is 1 m^2 and the thickness is 1 m so that the reservoir volume is 1 m^3.

3. Thickness:

Thickness is represented by triangular PDF in this model as seen in Figure 34 based on the related literature [56, 57, 58, 60]. To take the uncertainty into account, minimum thickness is defined as the total thickness of the cap rock and the reservoir rock. Most likely one is assigned as the total of minimum thickness and one more formation which underlies reservoir rock. Maximum values are defined as the total of minimum thickness and all formations, given in the generalized columnar section in Figure 18, that underlie the reservoir rock. For EGS, Kozak pluton is the reservoir rock whereas Yuntdağ formation is the cap rock. On the other hand, for hydrothermal system, Yuntdağ-1 formation is the reservoir rock whereas Soma formation is the cap rock. A sample configuration is given in Figure 35.

Hou et al. (2015) presents the minimum thickness of the stratigraphic units encountered during borehole drilling in their study area for Kozak-EGS application as follows: Yuntdağ Volcanites-1 as 300 m and Soma formation as 200 m. The thickness of Kozak pluton and Kınık formation are given as unknown by Hou et al. (2015) so these values are taken as 800 m and 400 m respectively based on the data published by Avşar and Parlaktuna, (2015) [44]. Thus, the thickness of the reservoir is taken as 2150 m (min.), 2400 m (most likely), 2800 m (max.) for Kozak granodiorite based on the field data published by Hou et al. (2015) [29]. For Yuntdağ Volcanites, reservoir thickness is taken as 500 m, 1300 m, and 1950 m as minimum, most likely and maximum values, respectively [29].

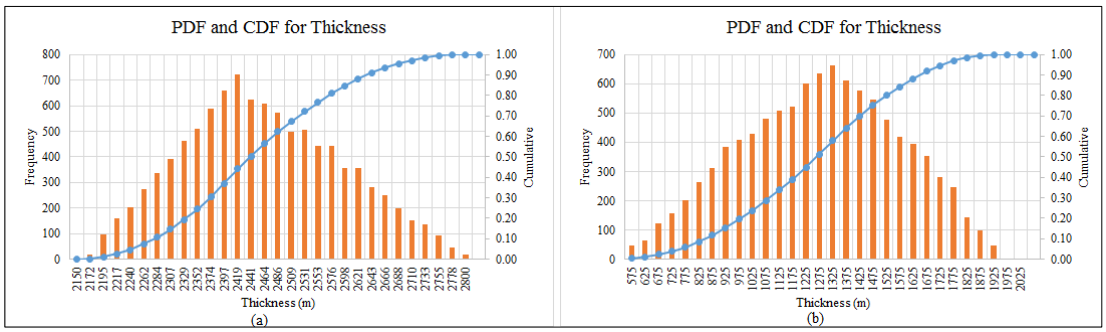

Figure 34: Histograms (as PDF) and cumulative expectation curves (as CDF) for thickness with triangular distribution: a) EGS b) Hydrothermal.

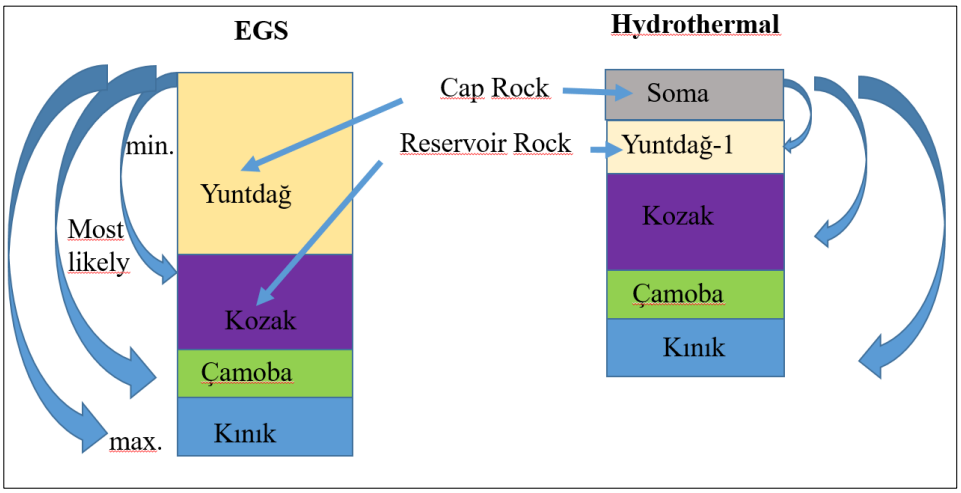

Figure 35: Illustration of formation sequences of Kozak-EGS and Yuntdağ hydrothermal system, explaining minimum, most likely and maximum cases for the input 'thickness' (not to scale).

4. Recovery Factor:

The recovery factor represents the amount of heat that is convected by fluid from the rock to the surface. Recovery factor is represented by triangular PDF in this model, as seen in Figure 36, based on related literature [54, 58, 60]. As suggested by Muffler and Cataldi (1977), the minimum, most likely and maximum values are taken as 0.07, 0.18 and 0.24, respectively [54].

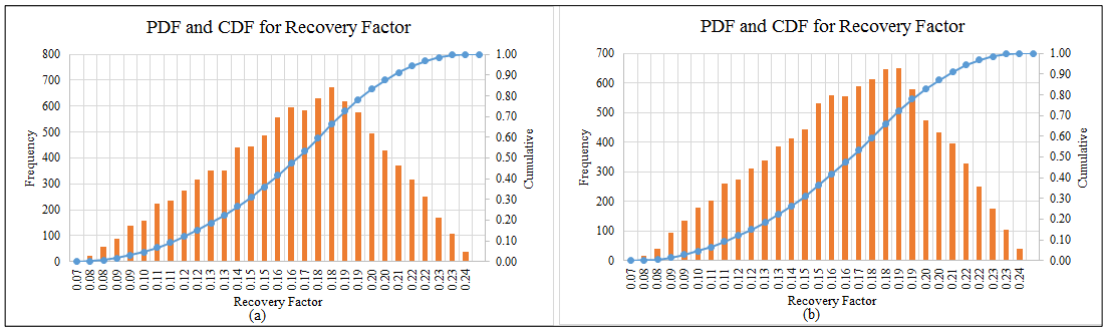

Figure 36: Histograms (as PDF) and cumulative expectation curves (as CDF) for recovery factor with triangular distribution: a) EGS b) Hydrothermal.

5. Rock-Fluid Temperature:

The rock-fluid temperature (RFT) is actually the reservoir temperature in geothermal resource assessment since rock and fluid are accepted as in equilibrium in terms of heat transfer. RFT is represented by triangular PDF in this model, as seen in Figure 37, based on the previous studies [56, 57, 58, and 60].

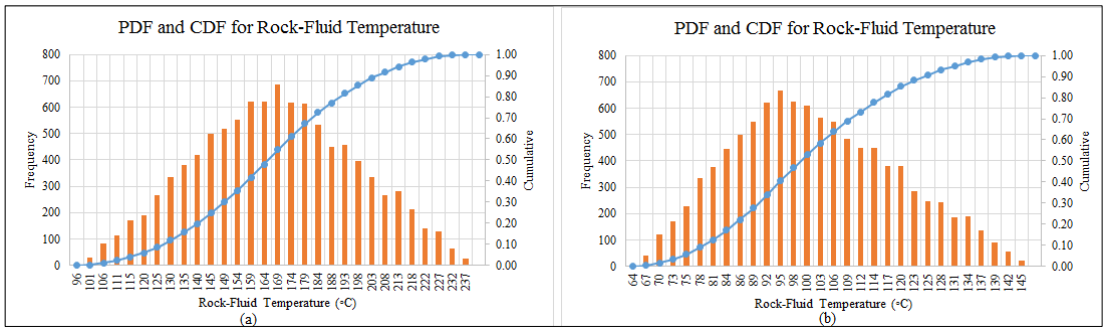

Figure 37: Histograms (as PDF) and cumulative expectation curves (as CDF) for rock-fluid temperature with triangular distribution: a) EGS b) Hydrothermal.

RFT is taken as 96 ºC, 165 ºC, 237 ºC as minimum, most likely, and maximum values respectively for Kozak granodiorite based on the cation geothermometer studies presented by Hou et. al., (2015). However, in this study, only the minimum (96 ºC) and the maximum (237 ºC) values were given with a standard deviation (28.6 ºC). The most likely value was calculated as 165 ºC by generating ranges that provide the closest standard deviation (28.78 ºC) to the given one. It is shown as bold in Table 8 that presents the steps in generation temperature range.

Table 8: Cation geothermometer results modified to get most likely value when calculated standard deviation is closest to the given standard deviation.

CATION GEOTHERMOMETER RESULTS				
Minimum (a)	Most likely (c)	Maximum (b)	STD. DEV. (Given)	STD. DEV. (Calculated)
96	100	237	28.6	32.77
96	105	237	28.6	32.23
96	110	237	28.6	31.71
96	115	237	28.6	31.24
96	120	237	28.6	30.80
96	125	237	28.6	30.40
96	130	237	28.6	30.04
96	135	237	28.6	29.72
96	140	237	28.6	29.45
96	145	237	28.6	29.22
96	150	237	28.6	29.04
96	155	237	28.6	28.91
96	160	237	28.6	28.82
96	161	237	28.6	28.81
96	162	237	28.6	28.80
96	163	237	28.6	28.79
96	164	237	28.6	28.79
96	**165**	**237**	**28.6**	**28.78**
96	170	237	28.6	28.79
96	175	237	28.6	28.85
96	180	237	28.6	28.96
96	185	237	28.6	29.11
96	190	237	28.6	29.31
96	195	237	28.6	29.56
96	200	237	28.6	29.84
96	205	237	28.6	30.18
96	210	237	28.6	30.55
96	215	237	28.6	30.97
96	220	237	28.6	31.42
96	225	237	28.6	31.91
96	230	237	28.6	32.44

For Yuntdağ hydrothermal system, RFT was assigned based on the available field data since all the wells presented in Table 6, are producing from hydrothermal reservoirs in Dikili. Cumulative distribution function of well bottom temperatures was plotted as can be seen in Figure 38. Then the well bottom temperature that corresponds to 50% probability was taken as most likely value (93 ºC). The minimum and maximum values were taken as 64.16 ºC and

145 ºC respectively based on the available well bottom temperature data, presented in Table 6 in Chapter 2.3.4.

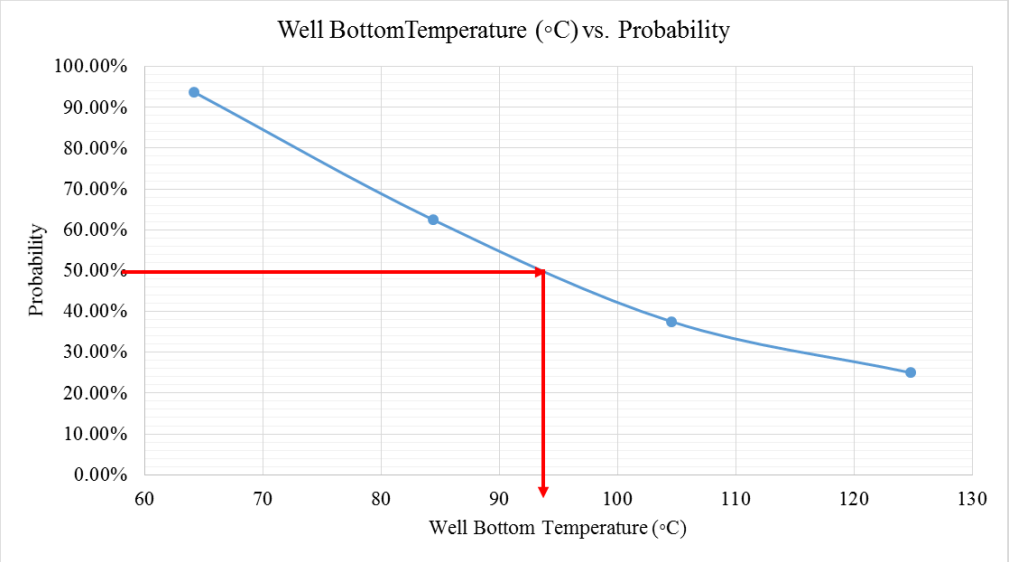

Figure 38: Cumulative expectation curve of well bottom temperatures.

6. Rock density:

Rock density is the only parameter that is represented by uniform distribution in this model. Because there was not any available rock density data measured in the field to assign as most likely value. Further, since andesite and granodiorite are both igneous rocks, the chance (i.e. frequency) to have any rock density value between the given range (minimum to maximum) is same. Figure 39 illustrates histograms (as PDF) and cumulative expectation curves (as CDF) for rock density with uniform distribution. For Kozak granodiorite, the density of the reservoir rock is taken as 2570 kg/m^3 (minimum) and as 2800 kg/m^3 (maximum). For Yuntdağ Volcanites, rock density is taken as 2500 kg/m^3 and 2800 kg/m^3 as minimum and maximum values, respectively, based on the data provided by literature [59].

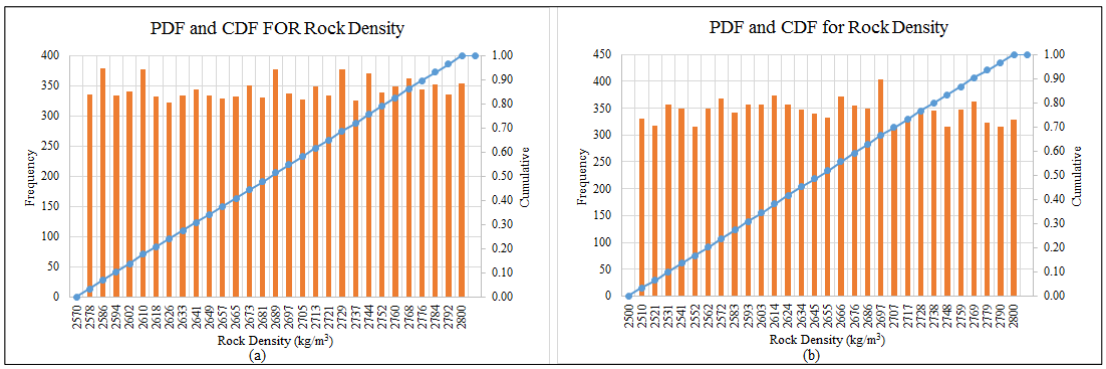

Figure 39: Histograms (as PDF) and cumulative expectation curves (as CDF) for rock density with uniform distribution: a) EGS b) Hydrothermal.

7. Fluid Density

Fluid density is represented by triangular PDF in this model, as seen in Figure 40, based on previous studies [57, 58]. There are three parameters that affect fluid density. These are pressure, temperature and salinity [61]. Since the depth (which affects the hydrostatic pressure) of reservoirs, salinity of water and expected reservoir temperature range are different for Kozak-EGS and Yuntdağ hydrothermal system, fluid density has been calculated separately for both cases.

For Kozak granodiorite hot dry rock system, depth of the reservoir is 1970 m (6461.6 ft) as explained earlier in 'thickness' section. With a pressure gradient of 0.433 psi/ft, the hydrostatic pressure will be 2798 psi. Since this reservoir is a hot dry rock, the reservoir fluid will be the fresh water injected from surface. Thus, the density of the fluid in reservoir formation is taken as 830 (min.), 905 (most likely), 965 (max.), in units of kg/m^3 considering that injected water is fresh water and hydrostatic pressure is 2798 psi [61].

For hydrothermal systems in Dikili, Alacalı and Yılmazer, (2005), state salinity (i.e. total dissolved solids) as 3000 ppm [62]. Depth of the reservoir is taken as 1420 m, consistent with the thickness data presented earlier in this chapter. Thus, hydrostatic pressure is obtained as 2017 psi according to a pressure gradient of 0.433 psi/ft. Then for Yuntdağ Volcanites, fluid density values are obtained from related charts (Figure 41) as 945 kg/m^3, 980 kg/m^3 and 995 kg/m^3 as minimum, most likely and maximum values, respectively [61].

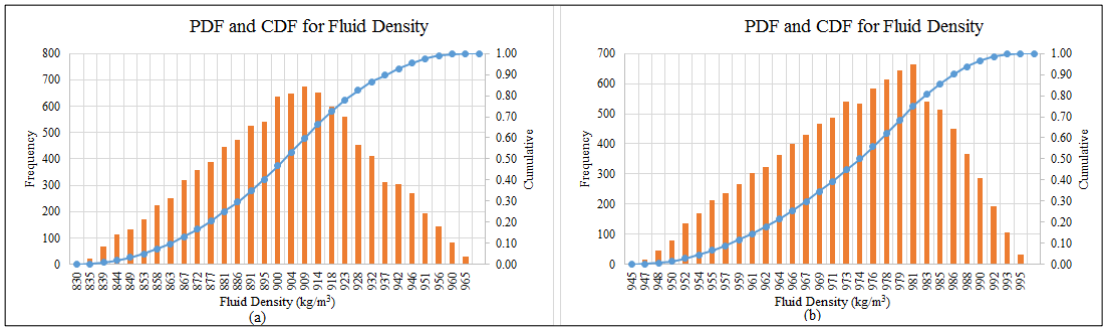

Figure 40: Histograms (as PDF) and cumulative expectation curves (as CDF) for fluid density with triangular distribution: a) EGS b) Hydrothermal.

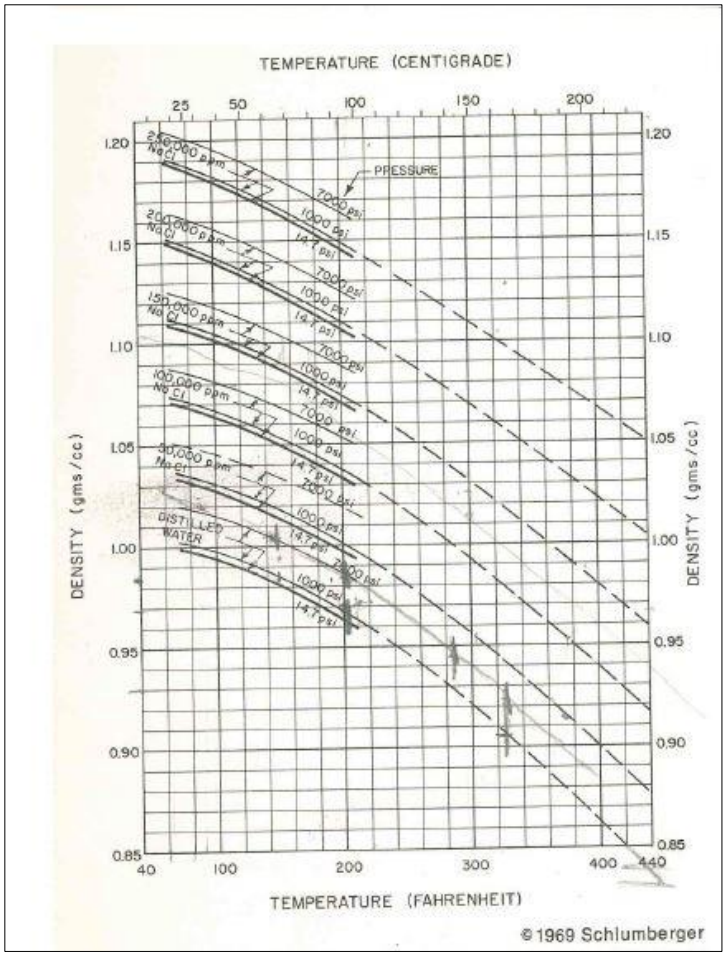

Figure 41: Fluid density chart for different salinity, temperature and pressure values [61].

In addition to the aforementioned parameters with PDFs, there are six input parameters that are constant. These are project life, load factor, conversion factor, specific heat capacity of rock, specific heat capacity of fluid and fluid utilization temperature (i.e. rejection temperature).

Project life is generally assumed to be 30 years [63]. For the unit conversion, it is taken as 9.46x108 seconds in the calculations.

For heating purposes, **load factor** is taken as 0.50 since the heating systems are needed in Dikili for six months as explained in Chapter 2.3. For electricity generation, power plants are active except the maintenance time since geothermal can provide base load. Thus, load factor is taken as 0.95 for indirect utilization [63].

For this study, **conversion factor** is taken as 0.12 for indirect utilization and as 0.95 for direct utilization.

Specific heat capacity of rock is taken for andesite for Yuntdağ reservoir as 0.965 kJ/kg-ºC and for granodiorite for Kozak reservoir as 1090 kJ/kg-ºC [59].

Specific heat capacity of water is taken as 4.26 kJ/kg-ºC corresponding to most likely temperature value that is 165 ºC for Kozak-EGS. For Yuntdağ hydrothermal system, specific heat capacity of water is taken as 4.14 kJ/kg-ºC that corresponds to 93 ºC which is the most likely reservoir temperature of this system.

Fluid utilization temperature for heating purposes case is taken as 41.5 ºC as it is the minimum well temperature in the region. For electricity production case, rejection temperature is taken as 60 ºC considering the possibility of scaling under this temperature.

Since these parameters are known exactly (like load factor) or do not change significantly (like specific heat capacity), they are taken as constants. For example, specific heat capacity of water only changes from 4.21 kJ/kg-ºC to 4.74 kJ/kg-ºC (i.e. about 0.5 kJ/kg-ºC) while the temperature changes from 96 ºC to 237 ºC as the minimum and maximum reservoir temperature of Kozak-EGS. Even if specific heat capacity is represented by triangular distribution in the model, it will not change the result significantly.

3.2.3. Geothermal Resource Development Scenarios

Considered scenarios are illustrated in Figure 42. Input parameter tables are given for real volume cases. The only difference between real volume and unit volume cases is that the area and the thickness of reservoir are 1 m^2 and 1 m, respectively in unit volume case.

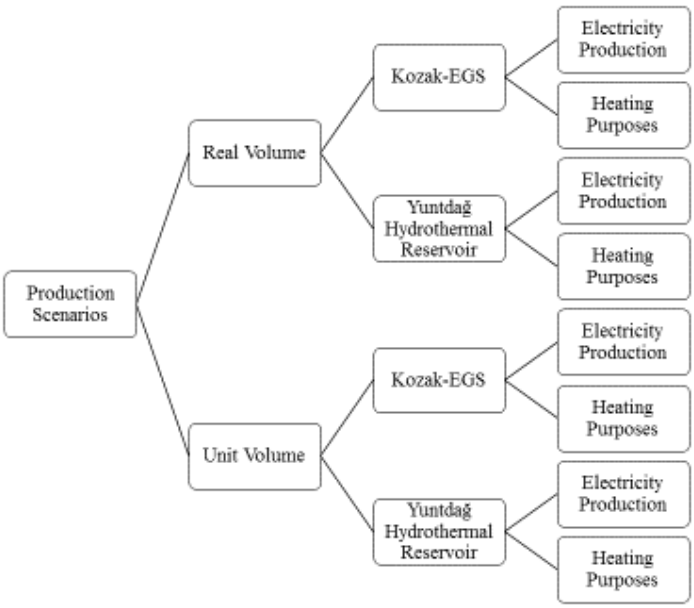

Figure 42: Developed scenarios considering different utilization ways of both real and unit volume of Yuntdağ and Kozak reservoirs.

1. Utilization of Kozak Pluton for Electricity Production

For the calculation of indirect utilization, which is electricity production, of Kozak granodiorite hot dry rock reservoir, the input parameters entered in the model are presented in Table 9.

Table 9: Input parameters for indirect utilization of Kozak Granodiorite hot dry rock reservoir.

	Unit	PDF	min.(x_l)	(x_m)	max.(x_h)	x_r
Porosity		Triangular	0.01	0.0200	0.03	0.50
Specific Heat Capacity of Rock-Granodiorite	kJ/kg°C	Constant		1.090		
Rock Density-Granodiorite	kg/m^3	Uniform	2570.00		2800.00	-11.17
Area	m^2	Triangular	3.30E+05	8.80E+05	2.21E+06	0.29
Thickness	m	Triangular	2150.00	2400.00	2800.00	0.38
Rock-Fluid Temperature	°C	Triangular	96.00	165.00	237.00	0.49
Fluid Utilization Temperature	°C	Constant		60.00		
Specific Heat Capacity of Fluid	kJ/kg°C	Constant		4.26		
Fluid Density	kg/m^3	Triangular	830.00	905.00	965.00	0.56
Recovery Factor		Triangular	0.07	0.18	0.24	0.65
Project Life	seconds	Constant		946080000.00		
Load Factor		Constant		0.96		
Conversion Factor		Constant		0.12		

2. Utilization of Kozak Pluton for Heating Purposes

For the calculation of direct utilization, which is district heating, of the Kozak granodiorite hot dry rock reservoir, the input parameters entered in the model are presented in Table 10.

Table 10: Input parameters for direct utilization of Kozak Granodiorite hot dry rock reservoir.

	Unit	PDF	min.(x_l)	(x_m)	max.(x_h)	x_r
Porosity		Triangular	0.01	0.0200	0.03	0.50
Specific Heat Capacity of Rock-Granodiorite	kJ/kg°C	Constant		1.090		
Rock Density-Granodiorite	kg/m^3	Uniform	2570.00		2800.00	-11.17
Area	m^2	Triangular	3.30E+05	8.80E+05	2.21E+06	0.29
Thickness	m	Triangular	2150.00	2400.00	2800.00	0.38
Rock-Fluid Temperature	°C	Triangular	96.00	165.00	237.00	0.49
Fluid Utilization Temperature	°C	Constant		41.50		
Specific Heat Capacity of Fluid	kJ/kg°C	Constant		4.26		
Fluid Density	kg/m^3	Triangular	830.00	905.00	965.00	0.56
Recovery Factor		Triangular	0.07	0.18	0.24	0.65
Project Life	seconds	Constant		946080000.00		
Load Factor		Constant		0.50		
Conversion Factor		Constant		0.95		

2. Utilization of Yuntdağ Volcanites for Electricity Production

For the calculation of indirect utilization, which is electricity production, the input parameters entered in the model are presented in Table 11.

Table 11: Input parameters for indirect utilization of Yuntdağ Volcanites reservoir.

	Unit	PDF	min.(x_l)	(x_m)	max.(x_h)	x_r
Porosity		Triangular	0.01	0.0129	0.03	0.15
Specific Heat Capacity of Rock-Volcanites	kJ/kg°C	Constant		0.965		
Rock Density-Volcanites	kg/m^3	Uniform	2500.00		2800.00	-8.33
Area	m^2	Triangular	1.50E+07	3.00E+07	4.50E+07	0.50
Thickness	m	Triangular	500.00	1300.00	1950.00	0.55
Rock-Fluid Temperature	°C	Triangular	64.16	93.00	145.00	0.36
Fluid Utilization Temperature	°C	Constant		60.00		
Specific Heat Capacity of Fluid	kJ/kg°C	Constant		4.14		
Fluid Density	kg/m^3	Triangular	945.00	980.00	995.00	0.70
Recovery Factor		Triangular	0.07	0.18	0.24	0.65
Project Life	seconds	Constant		946080000.00		
Load Factor		Constant		0.96		
Conversion Factor		Constant		0.12		

3. Utilization of Yuntdağ Volcanites for Heating Purposes

For the calculation of direct utilization of Yuntdağ Volcanites, the input parameters entered in the model are presented in Table 12.

Table 12: Input parameters for direct utilization of Yuntdağ Volcanites reservoir.

	Unit	PDF	min.(x_l)	(x_m)	max.(x_h)	x_r
Porosity		Triangular	0.01	0.0129	0.03	0.15
Specific Heat Capacity of Rock-Volcanites	kJ/kg°C	Constant		0.965		
Rock Density-Volcanites	kg/m^3	Uniform	2500.00		2800.00	-8.33
Area	m^2	Triangular	1.50E+07	3.00E+07	4.50E+07	0.50
Thickness	m	Triangular	500.00	1300.00	1950.00	0.55
Rock-Fluid Temperature	°C	Triangular	64.16	93.00	145.00	0.36
Fluid Utilization Temperature	°C	Constant		41.50		
Specific Heat Capacity of Fluid	kJ/kg°C	Constant		4.14		
Fluid Density	kg/m^3	Triangular	945.00	980.00	995.00	0.70
Recovery Factor		Triangular	0.07	0.18	0.24	0.65
Project Life	seconds	Constant		946080000.00		
Load Factor		Constant		0.50		
Conversion Factor		Constant		0.95		

3.2.4. Monte Carlo Simulation

Monte Carlo simulation is a technique to model the probability of different outcomes on plenty number of trials using Excel or a similar program. The advantage of using Monte Carlo simulation is that it enables users to see all the possible outcomes so that allows for better decision making under uncertainty. It shows not only what could happen but also how likely each outcome is. Further, in Monte Carlo simulations, it is easy to see which inputs have the biggest effect on results [55]. The summary of a Monte Carlo simulation for the purposes of assessing the uncertainity in heat-in-place calculations is as follows:

- Assign the probability distribution patterns of input parameters.
- Generate a set of values of each input variables with PDFs.
- Calculate heat in place.
- Repeat the above steps for a sufficient number of trials (i.e. iteration number, number of simulation) so that heat in place does not change significantly with further trials.

- Perform a frequency distribution study (i.e. cumulative expectation curve) based on the obtained heat in place [55].

3.3. Analysis

There are two different analyses carried out in this study. The first one is the impact analysis to find out which input parameter affects the output most. The second one is the critical analysis based on environmental and economical evaluation of the discussed systems.

3.3.1. Impact Analysis

In this study, geothermal resource assessment was done by applying volumetric method. Microsoft EXCEL was used to carry out Monte Carlo simulation to determine the stored energy and producible heat energy. In the model, porosity, area, thickness, fluid density, recovery factor and rock-fluid temperature are defined with triangular probability density functions, whereas rock density parameter is defined with uniform probability density function. All other input parameters (specific heat capacity of rock, specific heat capacity of fluid, fluid utilization temperature, project life, load factor and conversion factor) are defined as constant values. Among these input parameters the ones with uncertainty are tested to see which input parameter contributes the most to the variability of the outcome i.e. net electrical or thermal power so that the decision maker should focus on. This sensitivity analysis was done by plotting tornado diagrams. Tornado diagram is a kind of bar chart where the parameters are ordered vertically. Base case line that is seen as thick black solid line is obtained when all the parameters are taken as most likely values. Right hand sides of the tornado charts (colored as orange in electronic copies) represent the change in output when the maximum value of each input is considered. Similarly, left hand side of graphs, colored as blue in electronic copies, represent the change in the output when the minimum values of parameters are considered. Its aim is to show which item contributes most to the variability of the outcome, which can be identified with the length of the bar that corresponds to the input variable. Figure 43 presents a sample tornado chart generated for heating scenario for Yuntdağ hydrothermal system when real volume case is considered. Horizontal axis represents the net thermal power as output in units of MW_t. Vertical axis presents seven input parameters that are represented by PDFs in the model.

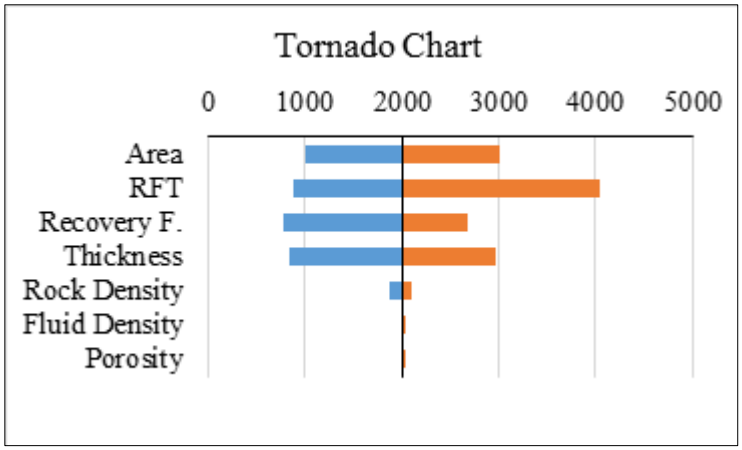

Figure 43: Sample Tornado chart (net thermal power in MW_t vs. input parameters with statistical distribution)

3.3.2. Critical Analysis

The sustainability attributes of the discussed systems are examined in terms of saved CO_2 amount employing proposed geothermal systems rather than fossil fuels, such as natural gas, and saved amount of money by employing a domestic resource rather than an imported energy source i.e. natural gas. Especially natural gas was used in comparison since the current electrical power is supplied from Bergama transformer station [65] by natural gas cycle plants in the region [6].

Considering the fact that the main player in Turkish electricity production market is natural gas with a 31.9% share [66], the annual amount of saved CO_2 is calculated.

All the calculations are done for indirect utilization of Kozak and Yuntdağ reservoirs' real volume cases.

The assumptions are as follows:

- Complete combustion is assumed to occur.
- Natural gas is totally composed of methane (CH_4).
- 1 joule= 0.239 cal.
- Combustion of 1 m^3 natural gas yields 8,250 kcal energy [67].
- Density of natural gas is equal to 0.7 kg/m^3 [68].
- All the CO_2 released directly to atmosphere without any capture.

Natural gas, which is mainly CH_4 i.e. methane, combustion reaction with oxygen is as follows:

$CH_4+2O_2 \rightarrow CO_2+2H_2O$

To calculate the overburden, the assumptions are as follows:

- As of 2016, based on European Union natural gas import prices, 1000 m^3 of natural gas costs 175 dollars [69].
- There is no CO_2 incentive or tax regulation taken into account as it is now in Turkey [70]. However, a CO_2 tax regulation such as 13.6 euro per ton of CO_2 [71] is also considered for a possible future scenario since Turkey has been working on it [70].
- The efficiency of the natural gas cycle power plant is 50%.

CHAPTER 4

RESULTS AND DISCUSSION

A Microsoft EXCEL based model was developed to determine the stored energy and the producible heat energy of Dikili geothermal field. To do this, firstly, the behavior of such a system was assumed to be described by probability density functions. Next, each input parameter with uncertainty was represented by a triangular or uniform probability density function and others were kept as constant values in the model. Further, 100, 200, 500, 1000, 2000, 5000 and 10,000 iterations are experimented in Monte Carlo simulation. The net power output was calculated for each discussed conditions by using the equations (3.1), (3.2), (3.3) and (3.4). Then the input parameters having the greatest impact on power output were determined by a sensitivity analysis employing tornado charts. Finally, a critical analysis including environmental and economical point of views was conducted to specify the sustainability attributes of the present research.

4.1. Sensitivity to the Number of Simulations

After experimenting different number of iterations, it was observed that the difference among the cases is less than or equal to 5 percent, as seen in Table 13. In other words, 100 and higher number of iterations yield in very close results as can be seen from the expectation curves presented in Figure 44. Nevertheless, 100 and 200 number of iterations are not capable of representing the assigned distributions. It is clearly seen in Figure 45 as histogram (PDF) and cumulative distribution function (i.e. S-curves are not smooth). Considering the fact that simulation for a single case is not computationally demanding, the number of the simulations is determined as 10,000 to maximize the accuracy.

Table 13: Power output (in units of MW_e) with P10, P50, P90 estimates for changing iteration numbers (the considered case here is the electricity production from the real volume of Kozak-EGS)

Iteration #	10%	50%	90%
100	32.8	17.5	8
200	33	17	8
500	33	17.5	8.5
1000	32	17	8.2
2000	31.3	17	8.5
5000	32	17	8
10000	32	17	8

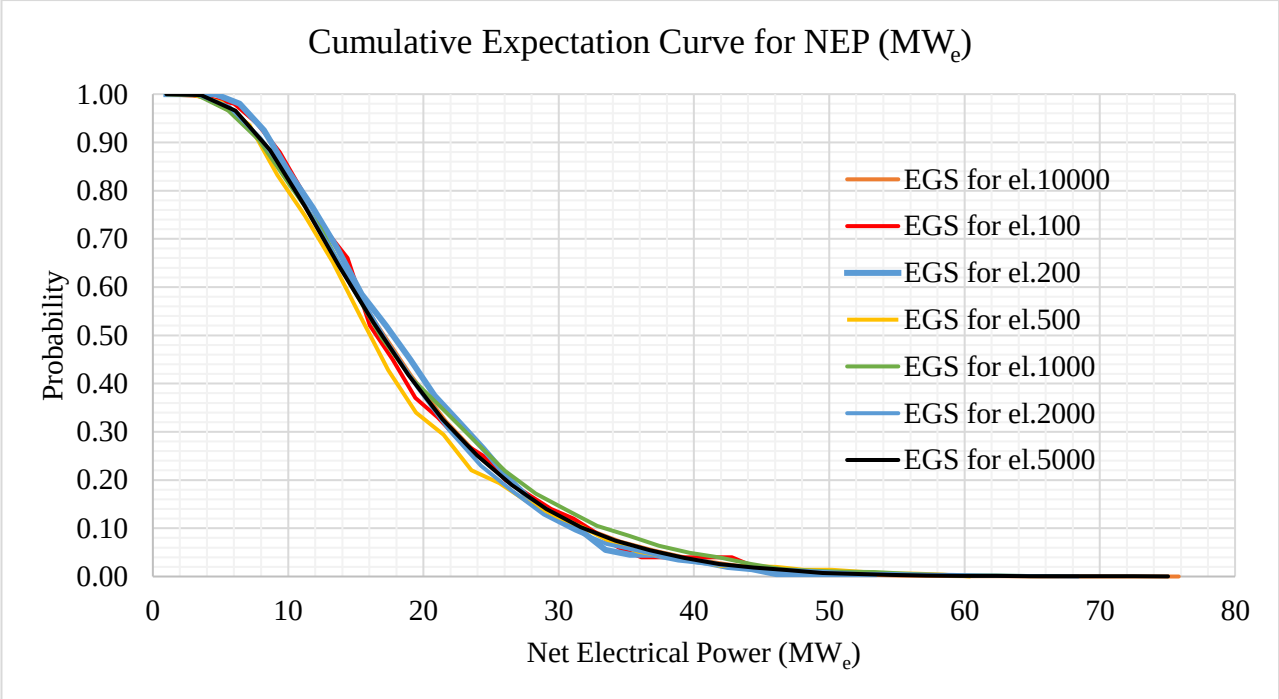

Figure 44: Cumulative expectation curves of calculated net electrical power (NEP) in units of MWe when 500, 1000, 2000, 5000 and 10,000 iterations are done in Monte Carlo simulation.

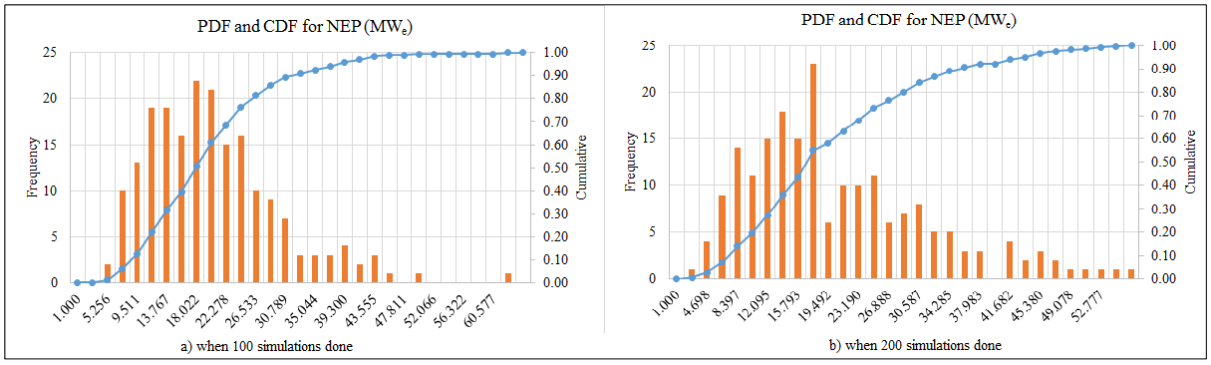

Figure 45: Cumulative expectation curves of calculated net electrical power (NEP) in units of MW_e when 100 and 200 iterations are done in Monte Carlo simulation.

4.2. Cumulative Distribution Function Curves and Results (P10, P50, P90 estimates)

Overall obtained results for real volume case are summarized in Table 14 and they are read from related plots presented in Figure 46, Figure 47, Figure 48 and Figure 49.

Table 14: Power output of each case in units of MW, with 10%, 50% and 90% probability, respectively (for real volume of reservoirs).

	P10	P50	P90
EGS-electricity	32	17	8
EGS-heating	560	300	150
Hydrothermal-electricity	150	75	30
Hydrothermal-heating	3148	1700	850

If unit volume (considered as 1 m^3) of reservoirs is considered, with P90, EGS can produce $7.2*10^{-8}$ MW_t and $3.8*10^{-9}$ MW_e whereas hydrothermal system can produce $2.8*10^{-8}$ MW_t and $1.0*10^{-9}$ MW_e. It shows that EGS can produce 2.6 fold of what hydrothermal system can produce in terms of thermal power. That amount is increasing up to 3.8 when electricity production is considered. In addition to P90 estimates, P10 and P50 estimates are given in Table 15.

Table 15: Power output of each case in units of MW, with 10%, 50% and 90% probability, respectively (for unit volume of reservoirs as 1 m^3).

	P10	P50	P90
EGS-electricity	1.01E-08	6.70E-09	3.80E-09
EGS-heating	1.72E-07	1.18E-07	7.20E-08
Hydrothermal-electricity	3.74E-09	2.10E-09	1.00E-09
Hydrothermal-heating	7.5E-08	4.80E-08	2.80E-08

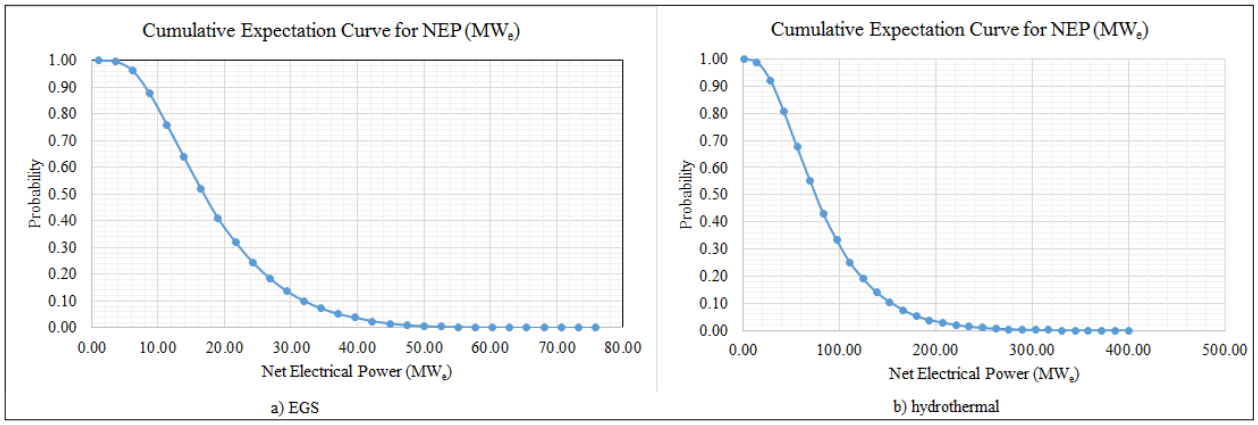

Figure 46: Cumulative expectation curve for indirect utilization of a) EGS b) hydrothermal reservoir for real volume case.

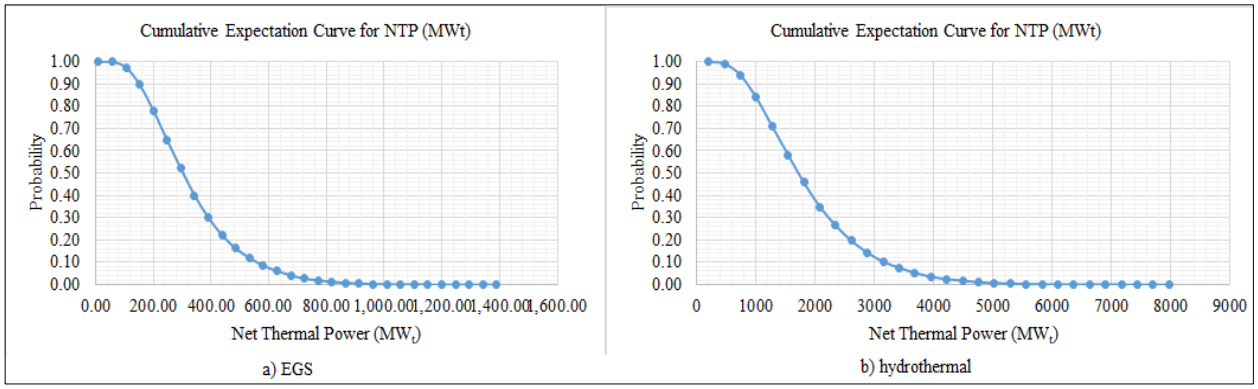

Figure 47: Cumulative expectation curve for direct utilization of a) EGS b) hydrothermal reservoir for real volume case.

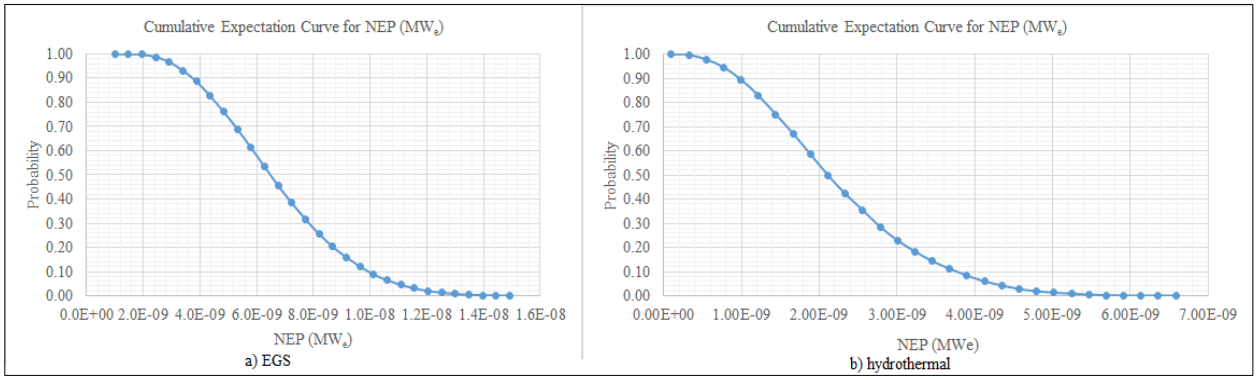

Figure 48: Cumulative expectation curve for indirect utilization of a) EGS b) hydrothermal reservoir for unit volume case.

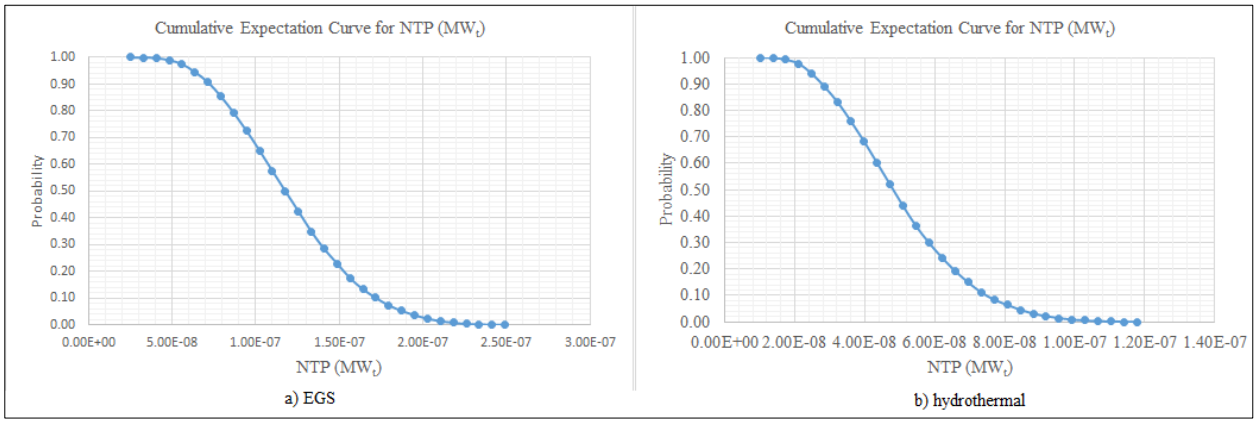

Figure 49: Cumulative expectation curve for direct utilization of a) EGS b) hydrothermal reservoir for unit volume case.

Previous work in this area focused on producing only from hydrothermal reservoirs. The present work extends the previous work by considering hot dry rock systems as an alternative reservoir. It compares the potential of aforementioned systems through different production scenarios as explained in Chapter 3.2.3.

4.3. Sensitivity Analysis of Heat Production to Input Parameters

Figure 50 presents tornado charts that reveal the sensitivity of heat potential to input parameters for real volume case. As seen, area of the reservoir and rock-fluid temperature (RFT) are the input parameters that have greatest impact on accessible resource base and the recoverable heat energy outputs. Recovery factor has also great effect, third ranked, on the output among seven parameters. Neither porosity nor fluid density has a significant impact on

the net electrical power output. However, for the unit volume case, rock-fluid temperature (RFT) and recovery factor have greatest effects on the output as seen in Figure 51. Rock density is the third ranked parameter having great effect on the output. Similar to the real volume case, neither porosity nor fluid density has a significant effect on the output. In unit volume case, as expected, area and thickness do not affect the result significantly since they are taken as constant, as 1 m^2 and 1 m respectively, to represent 1 m^3 unit volume.

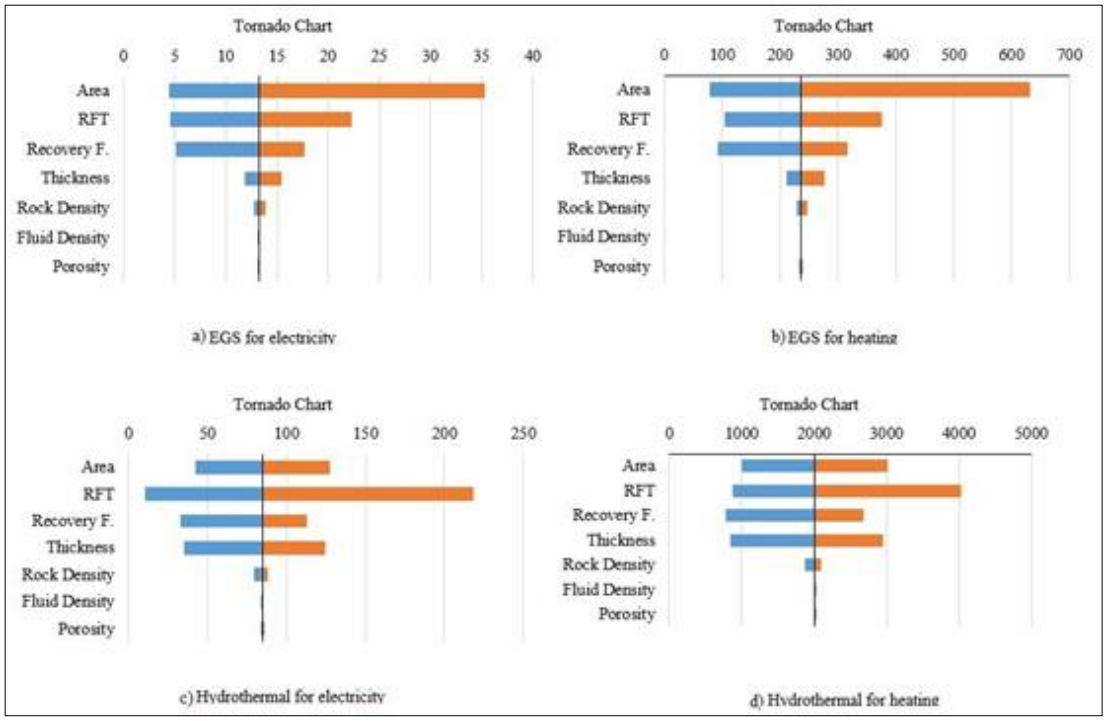

Figure 50: Sensitivity analysis for real volume case for four different production scenarios.

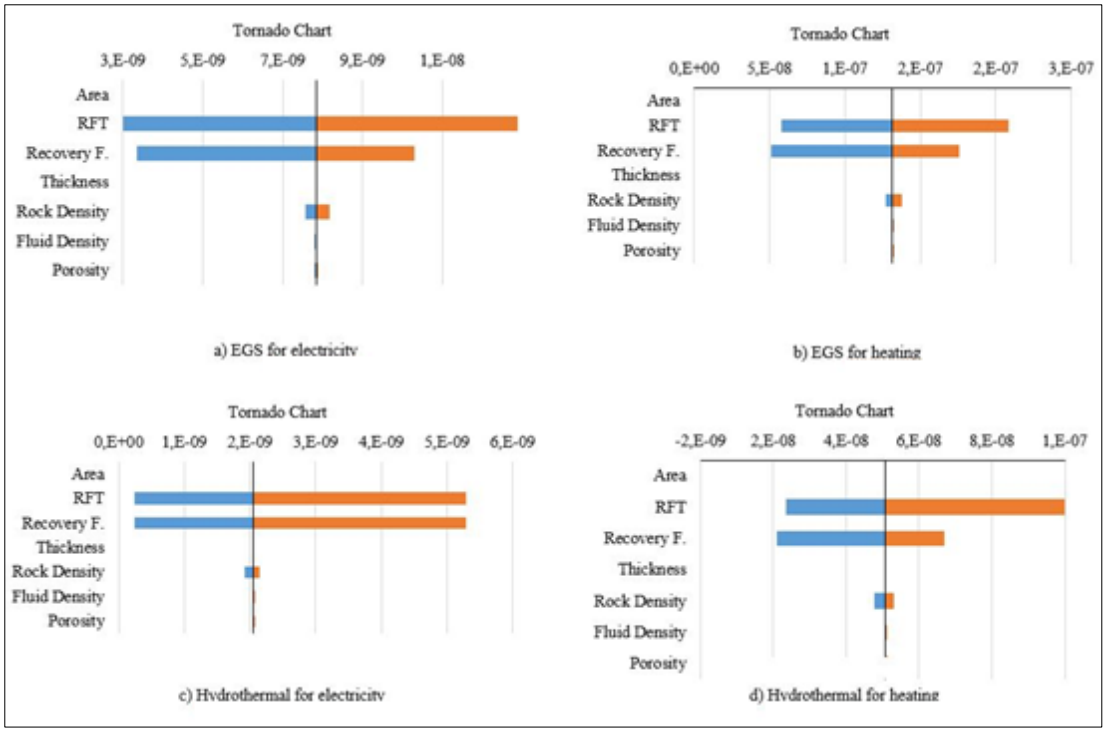

Figure 51: Sensitivity analysis for unit volume case for four different production scenarios.

4.4. Critical Analysis of the System

The sustainability attributes of the discussed systems are examined as follows:

- In terms of saved CO_2 amount (environmental point of view): by employing a renewable energy source such as geothermal rather than fossil fuels, such as natural gas.
- In terms of saved amount of money (economical point of view): by employing a domestic resource i.e. geothermal resources rather than an imported energy source i.e. natural gas.

4.4.1. Saved CO_2 Amount by Employing Proposed Geothermal Systems rather than Natural Gas

The annual amount of saved CO_2 is calculated as around 28,139 ton when 8 MW_e is produced from Kozak granodiorite and 105,519 ton when 30 MW_e is produced from Yuntdağ volcanites instead of natural gas.

Natural gas, which is mainly CH_4 i.e. methane, combustion reaction with oxygen is as follows:

$CH_4+2O_2 \rightarrow CO_2+2H_2O$

The molecular weight of methane is 12+ (4*1) =16 g

The molecular weight of CO_2 is 12+ (2*16) =44 g

It means that when 16 grams of natural gas is combusted, 44 grams of CO_2 is released to the atmosphere.

To convert 8 MW to kcal;

$8*10^6$ joules/sec *0.239 cal/joules $*10^{-3}$ kcal/cal = 1912 kcal/sec

To find the annual amount of saved CO_2;

1912 kcal/sec * 60*60*24*365 sec/year = 60,296,832,000 kcal in one year.

To find the amount of natural gas which can supply that much of energy;

60,296,832,000 kcal / 8250 kcal/m^3 = 7,308,706.909 m^3 natural gas.

To find the mass of natural gas, the volume is multiplied by the density of natural gas:

7,308,706.909 m^3 *0.7 kg/m^3 = 5,116,094.836 kg CH_4

As shown previously, 16 g CH_4 yields 44 g CO_2

5,116,094.836 kg CH_4 yields 5,116,094.836 * 44/16= 14,069,260.80 kg CO_2

If the efficiency of a natural gas cycle power plant is taken as 50%, then saved amount of CO_2 is doubled. It means that by using EGS rather than natural gas to generate 8 MW electricity, the annual amount of CO_2 saved is 28,138,521.60 kg. Results are given in Table 17.

Table 16: Basic steps and results of saved CO_2 amount calculation for electricity production from Kozak granodiorite EGS.

Calculation Steps	Results	Units
8 MW	8,000,000	J/s
1 joule	0.239	cal
1 cal	0.001	kcal
Seconds in year	31,536,000	sec/year
1 m^3 CH_4 in combustion	8,250	kcal
Density of natural gas	0.700	kg/m^3
CO_2 factor	2.750	44/16
Efficieny of power plant	0.500	
Paid per 1 m^3	0.175	$
8 MW	1,912	kcal/sec
Yearly kcal	60,296,832,000	kcal
Natural gas amount	7,308,706.91	m^3
Mass of natural gas	5,116,094.84	kg
CO_2 amount	14,069,260.80	kg
Saved CO_2	28,138,521.60	kg

Similarly, by using hydrothermal system rather than natural gas to generate 30 MW electricity, the annual amount of CO_2 saved is 119,588,716.80 kg. Related results are given in Table 17.

Table 17: Basic steps and results of saved CO_2 amount calculation for electricity production from Yuntdağ hydrothermal system.

Calculation Steps	Results	Units
30 MW	30,000,000	J/s
1 joule	0.239	cal
1 cal	0.001	kcal
Seconds in year	31,536,000	sec/year
1 m^3 CH_4 in combustion	8,250	kcal
Density of natural gas	0.700	kg/m^3
CO_2 factor	2.750	44/16
Efficieny of power plant	0.500	
Paid per 1 m^3	0.175	$
30 MW	7,170	kcal/sec
Yearly kcal	226,113,120,000	kcal
Natural gas amount	27,407,650.91	m^3
Mass of natural gas	19,185,355.64	kg
CO_2 amount	52,759,728.00	kg
Saved CO_2	105,519,456.00	kg

4.4.2. Saved Amount of Money by Employing a Domestic Resource rather than an Imported Energy Source

When it comes to the overburden on Turkish economy due to imported energy sources such as natural gas, generating 8 MW_e or 30 MW_e from domestic geothermal resources rather than imported natural gas saves 2,558,047.42 dollars or 9,592,677.82 dollars, respectively.
For real volume case;

Kozak Granodiorite HDR reservoir generates 8 MW_e;

2* 7,308,706.91 m^3/1000 m^3*175 $ = 2,558,047.42 $

Yuntdağ Volcanites hydrothermal reservoir generates 30 MW_e;

2* 27,407,650.91 m^3/1000 m^3*175 $ = 9,592,677.82 $

If unit volume case is also considered with an existing CO_2 tax regulation of 13.6 euro; annual amount of saved money changes as follows:

1. When the unit volume of reservoir is taken as 1 km^3, Kozak-EGS generates 3.8 MW_e. This saves 13,365,797.76 kg of CO_2 and 1,215,072.52 $ annually without any CO_2 tax case. With a CO_2 tax regulation like 13.6 euro per tons of CO_2 [74], annual saved amount changes to 1,394,174.206 $ from the operating companies' perspectives.

2. When the unit volume of reservoir is taken as 1 km^3, Yuntdağ hydrothermal system generates 1 MW_e. This saves 3,517,315.20 kg of CO_2 and 319,755.93 $ annually without any CO_2 tax case. With a CO_2 tax regulation like 13.6 euro per tons of CO_2, annual saved amount changes to 366,887.9564 $ from the operating companies' perspectives.

These facts highlight the sustainability attributes of the discussed systems in an environmental and economical point of views, respectively.

CHAPTER 5

CONCLUSIONS AND RECOMMENDATIONS

The present feasibility analysis consists of resource assessment, sensitivity analysis and critical analysis of the resource assessment's results in terms of sustainability. Resource assessment was carried out for low enthalpy Yuntdağ Volcanites hydrothermal system and hot dry rock Kozak pluton in Dikili by applying volumetric method. Heating and electricity production purposes were considered in the defined geothermal field yielding in four different production scenarios for real and unit volume cases separately. Sensitivity of the net power output to the number of the simulations was also tested. In the sensitivity analysis part, the impacts of input parameters on the outputs in the recoverable heat content calculation were ranked. In the critical analysis part, the findings of the present study were evaluated in terms of saved money and CO_2 amount by employing a domestic renewable energy source (geothermal) rather than an imported fossil fuel (natural gas). This thesis was also an opportunity to summarize what has been done and to suggest what should be done in Turkish geothermal energy sector. On the other hand, to our knowledge, it is the first academic study in Turkey that assesses the utilization of HDR reservoirs for electricity production. In these manners, the findings of this research are promising.

The main conclusions drawn from this thesis study are summarized as follows:

1. Net electrical power is 8 MW_e for a HDR system producing from Kozak granodiorite, with 90% probability. This amount increases to 17 MW_e, with 50% probability and to 32 MW_e, with 10% probability.
2. Net thermal power is 150 MW_t for a HDR system producing from Kozak granodiorite, 90% probability. This amount increases to 300 MW_t, with 50% probability and to 560 MW_t, with 10% probability.
3. Net electrical power is 30 MW_e for a hydrothermal system producing from Yuntdağ Volcanites, with 90% probability. This amount increases to 75 MW_e, with 50% probability and to 150 MW_e, with 10% probability.
4. Net thermal power is 850 MW_t for a hydrothermal system producing from Yuntdağ Volcanites, with 90% probability. This amount increases to 1700 MW_t, with 50% probability and to 3148 MW_t, with 10% probability.

5. Based on P90 estimates, only from hydrothermal, it is possible to make 4.2 times of today's net thermal production for real volume case. It corresponds to 4.17 million m^2 greenhouse heating or heating of 95,031 residences (one residence equivalence is assumed to be 100 m^2 floor area).
6. For unit volume case (considered as 1 m^3 reservoir), net electrical power is 3.80E-09 MW_e for a HDR system producing from Kozak granodiorite, with 90% probability. This amount increases to 6.70E-09 MW_e, with 50% probability and to 1.01E-08 MW_e, with 10% probability.
7. Net thermal power is 7.20E-08 MW_t for a 1 m^3 HDR reservoir producing from Kozak granodiorite, with 90% probability. This amount increases to 1.18E-07 MW_t, with 50% probability and to 1.72E-07 MW_t, with 10% probability.
8. Net electrical power is 1.00E-09 MW_e for a 1 m^3 hydrothermal reservoir producing from Yuntdağ Volcanites, with 90% probability. This amount increases to 2.10E-09 MW_e, with 50% probability and to 3.74E-09 MW_e, with 10% probability.
9. Net thermal power is 2.80E-08 MW_t for a 1 m^3 hydrothermal reservoir producing from Yuntdağ Volcanites, with 90% probability. This amount increases to 4.80E-08 MW_t, with 50% probability and to 7.50E-08 MW_t, with 10% probability.
10. Based on P90 estimates, for a given unit volume, Kozak-EGS can produce 2.6 times of what Yuntdağ hydrothermal reservoir can produce in terms of net thermal power. For net electrical power, Kozak-EGS can produce even 3.8 times of what Yuntdağ hydrothermal reservoir can produce.
11. No significant difference (less than or equal to five percent) is observed in the output when 500, 1000, 2000, 5000 and 10,000 iterations are applied.
12. Sensitivity analysis showed that the thickness and the area of the reservoir formation are the inputs that have greatest impact on accessible resource base and the recoverable heat energy outputs for real volume case.
13. Sensitivity analysis showed that the temperature and the recovery factor are the inputs that have greatest impact on accessible resource base and the recoverable heat energy outputs for unit volume case.
14. Sensitivity analysis showed that calculations are not sensitive to rock density, porosity and fluid density for neither real nor unit volume cases.
15. When the unit volume of reservoir is taken as 1 km^3, Kozak-EGS generates 3.8 MW_e. This saves 13,365,797.76 kg of CO_2 and 1,215,072.52 $ annually without any CO_2 tax case. With a CO_2 tax regulation such as 13.6 euro per tons of CO_2, annual saved amount changes to 1,394,174.206 $ from the operating companies' perspectives.

16. When the unit volume of reservoir is taken as 1 km^3, Yuntdağ hydrothermal system generates 1 MW_e. This saves 3,517,315.20 kg of CO_2 and 319,755.93 $ annually without any CO_2 tax case. With a CO_2 tax regulation such as 13.6 euro per tons of CO_2, annual saved amount changes to 366,887.9564 $ from the operating companies perspectives.

This presented study is a starting point for future academic studies and for investors who plans to set up a business in enhanced geothermal systems in Turkey. In the future with the required research and government promotion, these systems can be more popular and commercial. With the domestic equipment manufacturing, required project budgets may reduce. In developing nations such as Turkey, small scale clean energy plants can provide even larger benefits than large centralized power plants with job creation and less transmission loss. Further, increasing the geothermal share in Turkey's energy supply portfolio can also be a wise approach to increase the energy security.

Recommendations to improve the present study for future research are as follows:

1. The volumetric method, employed in this thesis, is not the only way to calculate the accessible resource base and recoverable heat energy of the study area. Further studies may employ magmatic heat budget method since it is capable of indicating accessible resource base only in volcanic regions and/or compare volumetric method to magmatic heat budget method to see the differences in the results.
2. In this model, density, porosity and specific heat capacity values of reservoir rocks are compiled from the literature. In the future, collecting samples from the field can be considered to increase the accuracy and to decrease the uncertainty of the input data. Thus a deterministic study can be done with the decreasing uncertainty and a numerical modelling study regarding the parameters changing with time such as pressure and temperature can be done with the increasing number of input parameters.
3. To determine the reservoir area more specifically, resistivity maps can be obtained through geophysical studies.
4. A further detailed feasibility study can employ not only recoverable heat energy stored in the reservoir rock but also additional constraints such as seismicity, proximity to transmission line corridor, water availability and a 'What-If' scenario for monetary cost.
5. It is possible to get a vector map of Turkey addressing the potential sites for HDR projects. Layers of such a map can be recent volcanism, high heat flow, localized

radiometric heat sources, seismicity, and water availability with different assigned weights.

6. Since the majority of the geothermal sites in Turkey are privatized, the current data are confidential and there is no access to them. That is why this study was conducted by employing the limited data. There should be a national database not only for geothermal but also for other energy sources which is free for research purposes. It can increase the quality and can enlarge the scope of the further research studies. Similarly, if there is a national system providing disposal of the data, it can encourage the investors even in a not-win case.

REFERENCES

[1] Grand challenges for engineering (pp. 1-6). (2008). National Academy of Sciences, on behalf of the National Academy of Engineering. Retrieved February 02, 2016, from http://www.engineeringchallenges.org/File.aspx?id=11574&v=ba24e2ed.

[2] United Nations, Department of Economic and Social Affairs, Population Division (2015). World Population Prospects: The 2015 Revision, World Population 2015 Wallchart. ST/ESA/SER.A/378.

[3] Türkiye Cumhuriyeti, Ekonomi Bakanlığı. (2016). Ekonomik Görünüm (p.9). Ankara.

[4] Türkiye Cumhuriyeti, Başbakanlık Devlet Planlama Teşkilatı, Yüksek Planlama Kurulu. (2009). Elektrik Enerjisi Piyasası ve Arz Güvenliği Strateji Belgesi (p. 9). Ankara.

[5] Türkiye Cumhuriyeti, Enerji Piyasası Düzenleme Kurumu, Strateji Geliştirme Dairesi Başkanlığı. (2015). Elektrik Piyasası 2014 Yılı Piyasa Gelişim Raporu (p. 5). Ankara.

[6] Güldar, S., (2014). İzmir İli Enerji Görünümü (2003-2014). TMMOB Elektrik Mühendisleri Odası İzmir Şubesi, Enerji Komisyonu.

[7] Şimşek, Ş. (2016). Türkiye Jeotermal Kaynaklar Haritası [Map].

[8] İklim Değişikliği Müzakereleri ve Türkiye. (n.d.). Retrieved August 29, 2016, from http://www.enerji.gov.tr/tr-TR/Sayfalar/Uluslararasi-Muzakereler.

[9] Yenilenebilir Enerji Kaynaklarının Elektrik Enerjisi Üretimi Amaçlı Kullanımına İlişkin Kanun, 1 § Birinci Bölüm-Amaç, Kapsam, Tanımlar ve Kısaltmalar (2010). 29/12/2010 tarihli ve 6094 sayılı Kanunun hükmü I Sayılı Cetvel.

[10] Yenilenebilir Enerji Kaynaklarının Elektrik Enerjisi Üretimi Amaçlı Kullanımına İlişkin Kanun, 9 § Beşinci Bölüm-Çeşitli Hükümler (2010). 29/12/2010 tarihli ve 6094 sayılı Kanunun hükmü I Sayılı Cetvel.

[11] Lally, M. (2011, August 10). U.S. Companies See Growth Potential in Turkey. Retrieved August 29, 2016, from http://www.renewableenergyworld.com/articles/2011/08/u-s-companies-see-growth-potential-in-turkey.html.

[12] Bertani, R. (2010). Geothermal Power Generation in the World. 2005–2010 Update Report. World Geothermal Congress, Bali, Indonesia.

[13] Bertani, R. (2015). Geothermal Power Generation in the World. 2010–2015 Update Report World Geothermal Congress, Melbourne, Australia.

[14] Mertoğlu, O., Simsek, S., and Basarir, N. Geothermal Country Update Report of Turkey (2010-2015), Proceedings World Geothermal Congress 2015, Melbourne, Australia, 19-25 April 2015.

[15] Jeotermal Kaynaklar ve Uygulama Haritası [Map]. (n.d.). In Maden Tetkik Ve Arama Genel Müdürlüğü Enerji Hammadde Etüt Ve Arama Dairesi Başkanlığı.

[16] Armstead, H. C. (1983). Geothermal energy: Its past, present, and future contributions to the energy needs of man. (2nd ed., pp. 377-388). NY or London: E. and F.N. Spon.

[17] Lund, J. W. and Boyd, T. L. (2015). Direct utilization of geothermal energy 2015 worldwide review, World geothermal congress, Melbourne, Australia.

[18] Elektrik Sahaları [Map]. (n.d.). In Maden Tetkik Ve Arama Genel Müdürlüğü Enerji Hammadde Etüt Ve Arama Dairesi Başkanlığı.

[19] Türkiye Cumhuriyeti Enerji Piyasası Düzenleme Kurumu, http://lisans.epdk.org.tr/epvys-web/faces/pages/lisans/elektrikUretim/elektrikUretimOzetSorgula.xhtml , last visited on September 2016.

[20] Lentz, A., and Almanza, R. (2006). Parabolic troughs to increase the geothermal wells flow enthalpy. ScienceDirect, solar energy (80), 1290-1295.

[21] Ulusal Tez Merkezi | Anasayfa. (n.d.). Retrieved February 02, 2016, from https://tez.yok.gov.tr/UlusalTezMerkezi/.

[22] What is Geothermal Energy? (n.d.). Retrieved August 30, 2016, from https://www.geothermal-energy.org/what_is_geothermal_energy.html.

[23] Tester, J. W., Drake, E. M., Driscoll, M. J., Golay, M. W., and Peters, W. A. (2005). Sustainable energy: Choosing among options. (pp. 491-499). London, England: MIT Press.

[24] Gupta, H., and Roy, S. (2007). Geothermal energy: An alternative resource for the 21st century. (1st ed., pp. 50-59). Netherlands.

[25] World's First Magma-EGS system created. (2014). Retrieved December 29, 2015, from http://iddp.is/wp-content/uploads/2014/01/News-in-English-16-01-2014.pdf .

[26] Fridleifsson, G. O., Albertsson, A., and Elders, W. A. (2010). 'Iceland Deep Drilling Project (IDDP) -10 Years Later- Still an Opportunity for International Collaboration', World Geothermal Congress, Bali, Indonesia.

[27] Gupta, H., and Roy, S. (2007). Geothermal energy: An alternative resource for the 21st century. (1st ed., pp. 57-58). Netherlands.

[28] Geothermal Technologies Compared. (2016). Retrieved August 30, 2016, from http://www.greenfireenergy.com/geothermal-technologies-compared.html.

[29] Hou, Z., Şen, O., Gou, Y., Eker, A. M., Li, M., Yal, G. P., Were, P. (2015). Preliminary geological, geochemical and numerical study on the first EGS project in Turkey. Environ Earth Sci Environmental Earth Sciences, 73(11), 6747-6767. doi:10.1007/s12665-015-4407-6.

[30] Aktif Tektonik Araştırma Grubu, http://www.atag.itu.edu.tr/v3/?p=135 , last visited on June 2012.

[31] Burçak, M. (2012). Kizgin Kuru Kaya (HDR: Hot Dry Rock) Ve Geliştirilebilir Jeotermal Sistemler (EGS: Enhanced Geothermal Systems), Maden Tetkik ve Arama Genel Müdürlüğü, Enerji Hammadde Etüt ve Arama Dairesi – Ankara.

[32] Burçak, M. (2015), Kizgin Kuru Kaya (KKK) Ve Geliştirilebilir Jeotermal Sistemler (GJS) Ve Türkiye'de Araştirmaya Uygun Bölgeler, MTA 80. Yıl Sempozyumu, Ankara, 03 Aralık 2015.

[33] Enerji Hammadde Etüt ve Arama Dairesi Başkanlığı. (2012). Türkiye jeotermal kaynak potansiyeli ve MTA genel müdürlüğü çalışmaları. Ankara, Türkiye: Maden Teknik Arama Genel Müdürlüğü.

[34] Gupta, H., and Roy, S. (2007). Geothermal energy: An alternative resource for the 21st century. (1st ed., pp. 11). Netherlands.

[35] Colorado Geological Survey, http://coloradogeologicalsurvey.org/energy-resources/geothermal-2/uses-2/electrical-generation/ , last visited on September 2016.

[36] Gürmat, http://www.gurmat.com.tr/en/index.php?p=fg&cat=143 , last visited on December 2013.

[37] Basel I. Ismail (2013). ORC-Based Geothermal Power Generation and CO_2-Based EGS for Combined Green Power Generation and CO_2 Sequestration, New Developments in Renewable Energy, Prof. Hasan Arman (Ed.), InTech, DOI: 10.5772/52063.

[38] Numov, http://www.numov.org/Praesentationen/geotermie/Cigir%20-%20Tuzla%20Jeotermal%20Enerji%20A.S..pdf , last visited on January 2014.

[39] Lund, J.W., and Boyd, T, L., "Direct Utilization of Geothermal Energy 2015 Worldwide Review", Proceedings World Geothermal Congress 2015, Melbourne, Australia, 19-25 April 2015.

[40] Csanyi, E. (Ed.). (2011, January 24). Geothermal Energy- The Hot Facts. Retrieved August 30, 2016, from http://electrical-engineering-portal.com/geothermal-energy-the-hot-facts.

[41] İklim: Dikili. (n.d.). Retrieved August 30, 2016, from http://tr.climate-data.org/location/25663/.

[42] Güneş Enerjisi Potansiyel Atlası. (n.d.). Retrieved August 30, 2016, from http://www.eie.gov.tr/MyCalculator/pages/35.aspx.

[43] Turan, A. (2015). 'Assessment of Geothermal and Solar Hybrid Power Generation Technologies in Turkey and Its Application to Menderes Graben', Proceedings World Geothermal Congress 2015, Melbourne, Australia, 19-25 April 2015.

[44] Parlaktuna, M., and Avşar, Ö. (2015). Evaluation of Dikili-Kaynarca Geothermal Field (NW Turkey). Proceedings World Geothermal Congress 2015, Melbourne, Australia, 19-25 April 2015.

[45] Özen, T., Tarcan, G. and Gemici, Ü. (2005). Hydrogeochemical Study of the Selected Thermal and Mineral Waters in Dikili Town, İzmir, Turkey. Proceedings World Geothermal Congress 2005, Antalya, Turkey, 24-29 April 2005.

[46] Özen, T., Tarcan, G., Gemici, Ü., ve AKSOY, N. (2008). Dikili-Bergama (İzmir) Termal Kaynaklarinin Hidrojeokimyasal Özellikleri Ve Kullanim Alanlari. Termal Ve Maden Sulari Konferansi, 24-25 Nisan 2008.

[47] MTA-JICA: Pre-Feasibility Study on the Dikili Bergama Geothermal Development Project in the Republic of Turkey. Final Report, M.T.A., Ankara, (1987).

[48] Kayan, İ, and Vardar, S. (2007). Physical geography of the Delta. The Madra River Delta: Regional Studies on the Aegean Coast of Turkey.

[49] Altunkaynak, Ş. and Yilmaz, Y. (1999), The Kozak Pluton and its emplacement. Geol. J., 34: 257–274. doi:10.1002/(SICI)1099-1034(199907/09)34:3<257::AID-GJ826>3.0.CO;2-Q.

[50] Bilim, F., Akay, T., Aydemir, A., and Kosaroglu, S. (2016). Curie point depth, heat-flow and radiogenic heat production deduced from the spectral analysis of the aeromagnetic data for geothermal investigation on the Menderes Massif and the Aegean Region, western Turkey. Geothermics, 60, 44-57. doi:10.1016/j.geothermics.2015.12.002.

[51] Tabar, E., Kumru, M., Saç, M., Içhedef, M., Bolca, M., and Özen, F. (2013). Radiological and chemical monitoring of Dikili geothermal waters, Western Turkey.

Radiation Physics and Chemistry, 91, 89-97. doi:10.1016/j.radphyschem.2013.04.037.

[52] Roba, C. A., Niţă, D., Cosma, C., Codrea, V., and Olah, Ş. (2012). Correlations between radium and radon occurrence and hydrogeochemical features for various geothermal aquifers in Northwestern Romania. Geothermics, 42, 32-46. doi:10.1016/j.geothermics.2011.12.001.

[53] Kalinci, Y., Hepbasli, A., and Tavman, I. (2008). Determination of optimum pipe diameter along with energetic and exergetic evaluation of geothermal district heating systems: Modeling and application. Energy and Buildings, 40 (5), 742-755. doi:10.1016/j.enbuild.2007.05.009.

[54] Muffler, P., & Cataldi, R. (1977). Methods for regional assessment of geothermal resources. doi:10.2172/6496850.

[55] Satter, Abdus Iqbal, Ghulam M. Buchwalter, James L.. (2008). Practical Enhanced Reservoir Engineering - Assisted with Simulation Software. PennWell.

[56] Sanyal, S. K., & Sarmiento, Z. (2005). Booking Geothermal Energy Reserves. GRC Transactions, 29.

[57] Atmaca, İ. (2010). RESOURCE ASSESSMENT IN AYDIN-PAMUKÖREN GEOTHERMAL FIELD (Master's thesis, Ankara/ Middle East Technical University, 2010) (pp. 48-82). Ankara.

[58] Avşar, Ö. (2011). GEOCHEMICAL EVALUATION AND CONCEPTUAL MODELING OF EDREMİT GEOTHERMAL FIELD. (Phd thesis, Ankara/ Middle East Technical University, 2011). Ankara.

[59] Schön, J. H., Physical properties of rocks. (2011) Elsevier.

[60] Arkan, S., Parlaktuna, M. (2005) Resource Assessment of Balçova Geothermal Field Proceedings World Geothermal Congress 2005, Antalya, Turkey, 24-29 April 2005.

[61] Schlumberger Log Interpretation Charts (1972 edition) (pp.47).

[62] Yılmazer, S., and Alacalı, M. (2005) Distribution of Hot Water Resources and Potentials of İzmir Province, Proceedings World Geothermal Congress 2005, Antalya, Turkey, 24-29 April 2005.

[63] Garg, S. K., & Combs, J. (2015). A reformulation of USGS volumetric “heat in place” resource estimation method. Geothermics, 55, 150-158. doi:10.1016/j.geothermics.2015.02.004.

[64] Simsek, S., Mertoğlu, O., Bakır, N., Akkuş, İ., and Aydoğdu, O., Geothermal Energy Utilisation, Development and Projections - Country Update Report (2000-

2004) of Turkey, Proceedings World Geothermal Congress 2005, Antalya, Turkey, 24-29 April 2005.

[65] Dikili Belediyesi, http://www.izmir-dikili.bel.tr/tr/dikili-hakkinda , last visited on August 2016.

[66] TC Enerji ve Tabii Kaynaklar Bakanlığı, (2011). Elektrik üretim sektör raporu.

[67] Engin Mühendislik, http://www.enginmuh.com/isitma_sistemleri_2.html , last visited on December 2012.

[68] Bilgin, A. (n.d.). Kazanlarda enerji verimliliği ve emisyonlar. Retrieved from Makina Mühendisleri Odası website: http://www.mmo.org.tr/resimler/dosya_ekler/1673a38f02b5852_ek.pdf.

[69] European Union Natural Gas Import Price Chart [Chart]. (2016). In Commodity Markets Review. World Bank. Retrieved September, 2016, from https://ycharts.com/indicators/europe_natural_gas_price.

[70] Kıvılcım, İ., (2014) Türkiye'nin Karbon Piyasalarındaki Mevcut Durumu, İKV Değerlendirme Notu, İktisadi Kalkınma Vakfı.

[71] Hotunluoğlu, H., ve Tekeli, R., (2007) Karbon Vergisinin Ekonomik Analizi ve Etkileri: Karbon Vergisinin Emisyon Azaltıcı Etkisi Var mı?, Sosyo-Ekonomi, Temmuz-Aralık, 2007-2.